# BRNO UNIVERSITY OF TECHNOLOGY

VYSOKÉ UČENÍ TECHNICKÉ V BRNĚ

## FACULTY OF ELECTRICAL ENGINEERING AND COMMUNICATION

FAKULTA ELEKTROTECHNIKY
A KOMUNIKAČNÍCH TECHNOLOGIÍ

## DEPARTMENT OF ELECTRICAL POWER ENGINEERING

ÚSTAV ELEKTROENERGETIKY

## SUBCHANNEL MODEL OF APR1400 REACTOR CORE

SUBKANÁLOVÝ MODEL AKTIVNÍ ZÓNY REAKTORU APR1400

### MASTER'S THESIS

DIPLOMOVÁ PRÁCE

**AUTHOR**　　　　　　Nurmet Kazimov
AUTOR PRÁCE

**SUPERVISOR**　　　　Ing. Štěpán Foral, Ph.D.
VEDOUCÍ PRÁCE

BRNO 2023

# BRNO FACULTY OF ELECTRICAL
# UNIVERSITY ENGINEERING
# OF TECHNOLOGY AND COMMUNICATION

# Master's Thesis

Master's study program **Electrical Power Engineering**

Department of Electrical Power Engineering

| | | | |
|---|---|---|---|
| *Student:* | Nurmet Kazimov | *ID:* | 233437 |
| *Year of study:* | 2 | *Academic year:* | 2022/23 |

**TITLE OF THESIS:**

## Subchannel model of APR1400 reactor core

**RECOMMENDED LITERATURE:**

Technická dokumentace reaktoru APR1400 na stránkách U. S. NRC a dle doporučení vedoucího diplomové práce.

| | | | |
|---|---|---|---|
| *Date of project specification:* | 6.2.2023 | *Deadline for submission:* | 22.5.2023 |

*Supervisor:* Ing. Štěpán Foral, Ph.D.

**prof. Ing. Petr Toman, Ph.D.**
Chair of study program board

# Abstract

The master thesis describes the subchannel analysis methodology. Subchannel analysis serves as a valuable tool in evaluating the safety of nuclear reactor operations. The results obtained from subchannel analysis provide vital information for assessing risks associated with boiling crises, as well as evaluating the effectiveness of moderation and fuel rod plutonium production. To achieve this, it is imperative to develop and validate an active zone model within the subchannel code. The master thesis deals with this procedure in the case of the active zone of the APR1400 reactor. The results are compared with experimental data and other simulation results to validate the accuracy of the model.

## Keywords

Subchannel analysis, APR1400, pressurized water reactor, Subchannel code, reactor model

# Abstrakt

Diplomová práce popisuje metodiku subkanálové analýzy. Subkanálová analýza slouží jako cenný nástroj při hodnocení bezpečnosti provozu jaderných reaktorů. Výsledky získané z analýzy subkanálů poskytují zásadní informace pro hodnocení rizika vzniku krize varu, stejně jako hodnocení účinnosti umírněnosti a produkce plutonia v palivových tyčích. Aby toho bylo dosaženo, je nezbytné vyvinout a validovat model aktivní zóny v v subkanálovém kódu. Diplomová práce se tímto postupem zabývá v případě aktivní zóny reaktoru APR1400. Výsledky jsou porovnány s experimentálními daty a dalšími výsledky simulace, aby validovat přesnost modelu.

## Klíčová slova

Subkanálová analýza, APR1400, tlakovodní reaktor, Subkanálový kod, model reaktoru

# Bibliographic citation

KAZIMOV, Nurmet. *Subkanálový model aktivní zóny reaktoru APR1400.* Brno, 2023. Dostupné také z: https://www.vut.cz/studenti/zav-prace/detail/149346. Diplomová práce. Vysoké učení technické v Brně, Fakulta elektrotechniky a komunikačních technologií, Ústav elektroenergetiky. Vedoucí práce Štěpán Foral.

# Author's Declaration

**Author:**                    *Nurmet Kazimov*

**Author's ID:**              *233437*

**Paper type:**              *Master's Thesis*

**Academic year:**        *2022/23*

**Topic:**                      *Subchannel model of APR1400 reactor core*

I declare that I have written this paper independently, under the guidance of the advisor and using exclusively the technical references and other sources of information cited in the project and listed in the comprehensive bibliography at the end of the project.

As the author, I furthermore declare that, with respect to the creation of this paper, I have not infringed any copyright or violated anyone's personal and/or ownership rights. In this context, I am fully aware of the consequences of breaking Regulation S 11 of the Copyright Act No. 121/2000 Coll. of the Czech Republic, as amended, and of any breach of rights related to intellectual property or introduced within amendments to relevant Acts such as the Intellectual Property Act or the Criminal Code, Act No. 40/2009 Coll., Section 2, Head VI, Part 4.

.
Brno, May 22, 2023                          ----------------------------------------
                                                               author's signature

# Acknowledgement

I would like to thank my supervisor Štěpán Foral for his invaluable advice and support in conducting this master thesis.

Brno, May 22, 2023            -------------------------------------------
                                                    Author's signature

# Contents

# INTRODUCTION

The aim of the master thesis was to get familiar with the technological features of the APR1400 reactor, introduce the basics of the subchannel analysis methodology, based on applied knowledge from the theoretical part create the model of the APR1400 reactor for subchannel analysis code ALTHAMC12 and validate the model against the published data.

In the first chapter, the main aim is to frame the theoretical framework of the APR1400 reactor. The chapter consists of a general description of the primary circuit, the reactor core and fuel. While in the second chapter, the method of subchannel analysis is explained. The thermalhydraulic subchannel analysis code ALTHAMC12 is introduced. The third chapter aims to describe the model of the APR1400 reactor core. And in the last chapter, the validation of the model against the published data is presented.

# 1. APR-1400 REACTOR

In this chapter provides a comprehensive overview of the APR1400 reactor design, its main characteristics of the primary system, reactor core, and fuel system.

The chapter introducing the main characteristics of the APR1400 reactor, including its thermal and electrical power output, design life, and type of coolant. The main attention is paid to the reactor core and its design, including the characteristics of fuel assemblies and fuel rods.

## 1.1 Main characteristics

The APR1400 reactor is a two-loop pressurized water reactor (PWR), developed in the Republic of Korea, based on innovative design improvements and technology enhancements built on the design, construction, operation, and maintenance of the *Optimized Power Reactor 1000* [5]. This advanced reactor is based on the System 80+ of the American company Combustion Engineering (CE). The main technical characteristics are indicated in Table 1 [3]. A schematic diagram of arrangements and locations of the primary components are shown in Figure 1 [3].

The major components of the primary circuit are a reactor vessel, two coolant loops, each containing one hot leg, two cold legs, one steam generator (SG), and two reactor coolant pumps (RCPs), and one pressurizer (PZR) connected to one of the hot legs. The APR1400 reactor adopted integrated head assembly (IHA) to provide lifting the reactor vessel closure head and its appurtenances, cooling of the control element drive mechanism [2].
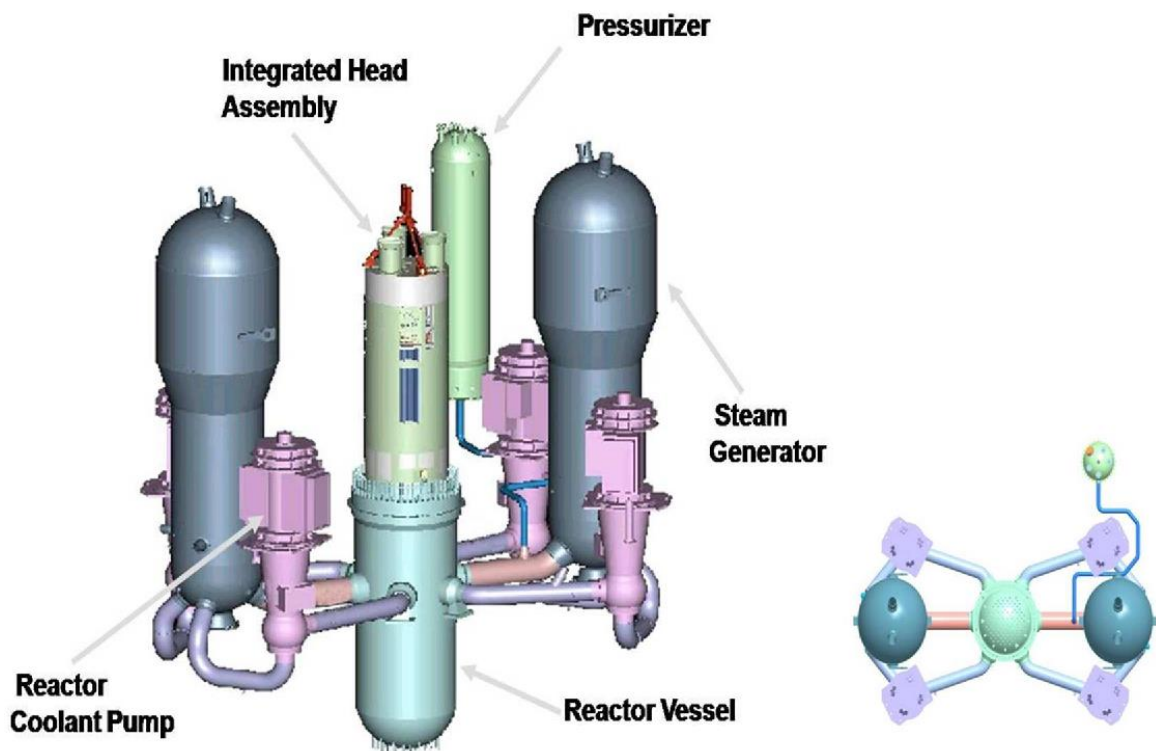


**Figure 1. Primary circuit of the APR1400 reactor design** [3]

Two steam generators and four reactor coolant pumps are arranged symmetrically. The steam generators are located on higher position than the reactor vessel for natural circulation. For vent and drain, the elevation of the PZR and the surge line is higher than that of reactor coolant piping.

The APR1400 reactor has several advanced features such as the direct vessel injection from the safety injection system, passive low regulation device in the safety injection tank, in-containment refueling water supply system, advanced safety depressurization system, and systems for severe accident mitigation and management. The advanced main control room, designed with the consideration of human factors engineering, with full-digital instrumentation and control (I&C) systems is another example of the design improvement.

Table 1. Main technical characteristics of the APR1400 reactor [3]

| Type of reactor | Pressurized Water Reactor (PWR) |
|---|---|
| Reactor thermal output | 3983 MWth |
| Power plant output, gross | 1455 MWe |
| Power plant output, net | 1400 MWe |
| Power plant efficiency, net | 35.1 % |
| Plant design life | 60 Years |
| Plant availability target > | 90 % |
| Seismic design, SSE | 0.3 |
| Primary coolant material | Light Water |
| Secondary coolant material | Light Water |
| Moderator material | Light Water |
| Thermodynamic cycle | Rankine |
| Type of cycle | Indirect |

Especially, the plant general arrangement has been improved with the reflection of operation and construction experiences of OPR1000.

The pressure vessel with internal structures is depicted in Figure 2. The main part of the reactor system is the pressure vessel with internal structures: core support structures, fuel assemblies, control rod assemblies, and control and instrumentation components.

The reactor pressure vessel is a vertically mounted cylindrical vessel with a hemispherical lower head welded to the vessel and a removable hemispherical closure head. The direct vessel injection (DVI) nozzles are attached to the reactor vessel for the direct emergency coolant injection as a part of the safety injection system. The dome and flange are welded together to form the upper closure head, on which the control element drive mechanism (CEDM) nozzles are welded. The core support structures, which include the core support barrel, upper guide structure assembly and lower support structure are designed to support and orient the reactor core fuel assemblies and control element assemblies, and to direct the reactor coolant to the core.
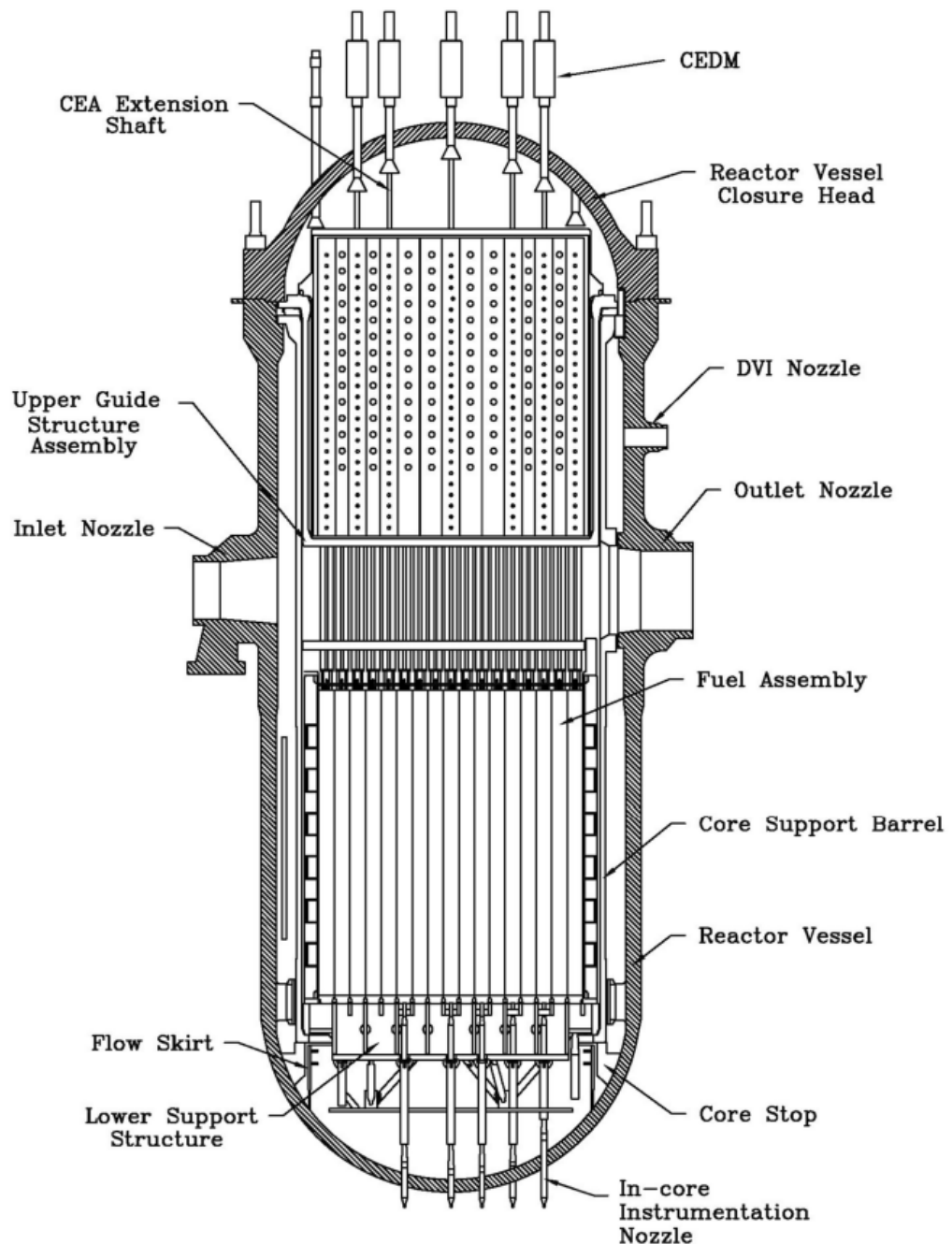
**Figure 2. General Assembly of the APR1400 reactor** [1]

## 1.2 Reactor core

The reactor core consists of 241 fuel assemblies made of fuel rods containing uranium dioxide (UO2) fuel. The number of control element assemblies (CEAs) used in the core is 93 in which 76 CEAs are full-strength reactivity control assemblies and the rest are part-strength CEAs. The main parameters of the reactor configuration are indicated in Table 2 [1]. The reactor core cross section is depicted in Figure 3 [1].

Table 2. Core configurations [1]

| Item | Value |
| --- | --- |
| Number of fuel assemblies in core, total | 241 |
| Number of CEAs | 93 |
| Number of fuel rod locations | 56.876 |
| Spacing between fuel assemblies, fuel rod surface to surface, cm | 0.549 |
| Spacing, outer fuel rod surface to core shroud, cm | 0.554 |
| Hydraulic diameter, nominal channel, cm | 1.264 |
| Total flow area (excluding guide thimble tubes), $m^2$ | 5.825 |
| Total core area, $m^2$ | 10.433 |
| Core equivalent diameter, m | 3.647 |
| Core circumscribed diameter, m | 3.873 |
| Total fuel loading, kg U (assuming all rod locations are fuel rods) | $103.82 \times 103$ ($228.9 \times 103$) |
| Total fuel weight, kg UO2 (assuming all rod locations are fuel rods) | $117.8 \times 103$ ($259.7 \times 103$) |
| Total weight of zirconium alloy, kg | 29.511 |
| Fuel volume (including dishes), $m^3$ | 11.42 |
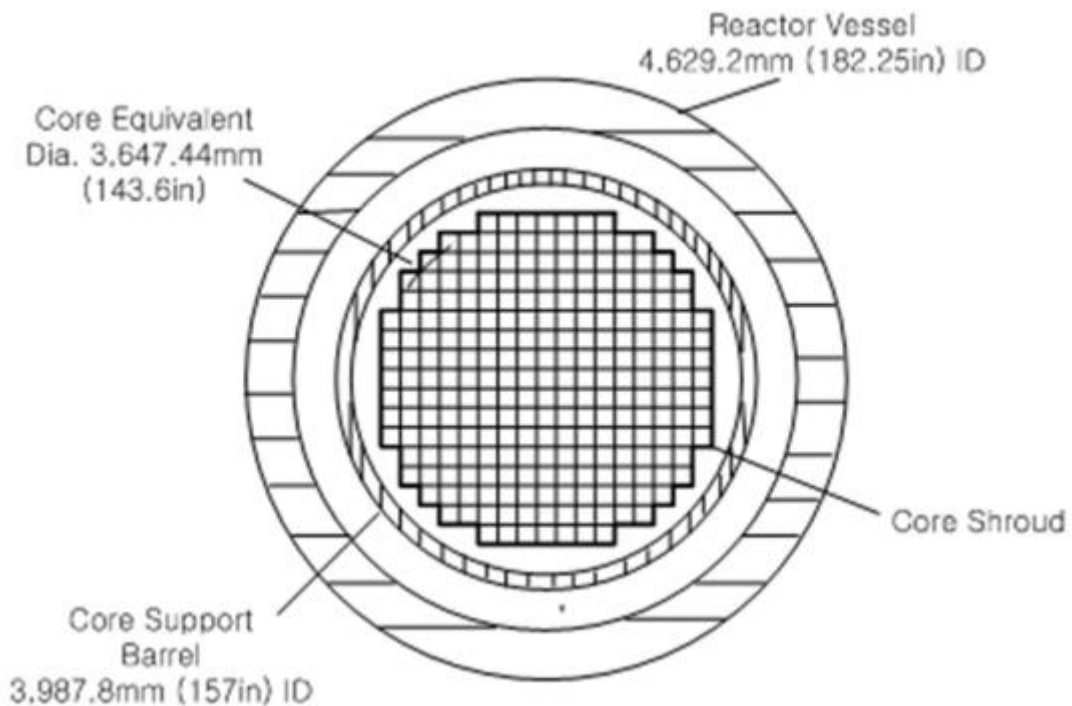


**Figure 3. The APR1400 reactor core cross section** [1]

With regards to the topic of the diploma thesis, special focus is given to core flow paths and bypass flows which are explained using Figure 4. The main coolant flow path in the reactor vessel is down the annulus between the reactor vessel and the core support barrel, through the flow skirt, up through the core support region and the reactor core, through the fuel alignment plate, and out through the two reactor vessel outlet nozzles. Some portion of the flow entering the reactor vessel is not effective for cooling the core. This portion is called the core bypass flow. Part of the bypass flow is used to cool the reactor internals in the areas not in the main coolant flow path and to cool the CEAs. Table 3 lists the bypass flow paths and the percentage of the total vessel flow that enters and leaves these paths.

Table 3. Reactor Coolant Bypass Flows [1]

| Bypass Path | Percentage of Total Vessel Flow, Design Maximum Value (Best Estimated Value) |
|---|---|
| Outlet nozzle clearances | 1.4 (1.1) |
| Alignment keyways | 0.5 (0.4) |
| Core shroud annulus | 0.4 (0.3) |
| Guide tubes | 0.7 (0.6) |
| Total bypass | 3.0 (2.4) |
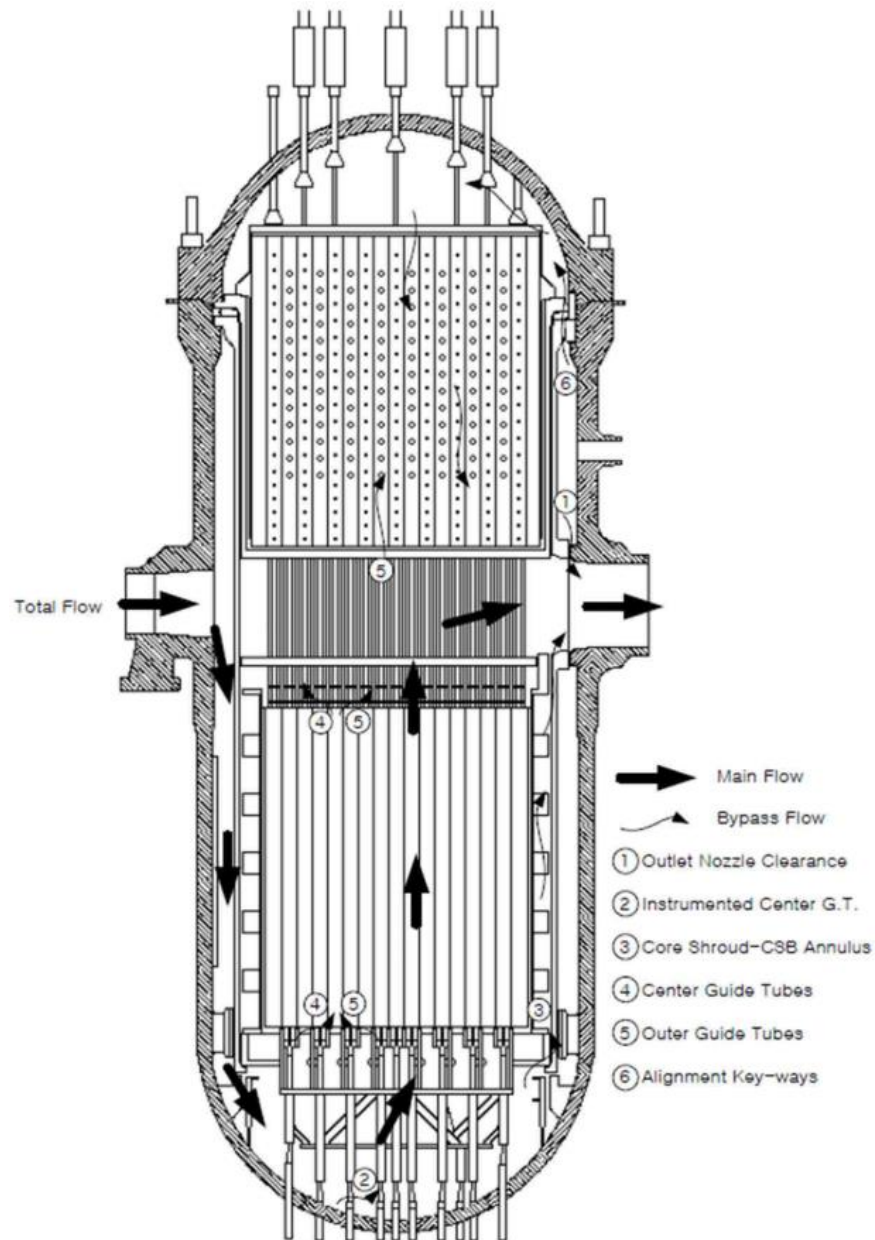
**Figure 4. Reactor Coolant Flow Paths Diagram**

### 1.3 Fuel system

The fuel assembly consists of 236 fuel rods and burnable absorber rods, 4 guide thimbles, 1 instrument tube, 12 grids, 1 top nozzle, and 1 bottom nozzle. The guide thimbles, grids, top nozzle, and bottom nozzle form the structural frame of the assembly. A schematic diagram of the fuel assembly is shown in Figure 5.

The advanced fuel assembly, named as PLUS7, provides enhanced thermal hydraulic and nuclear performance and the structural integrity. Mechanical design parameters of fuel assemblies, grids and fuel rod are shown in Tables 4 and 5.
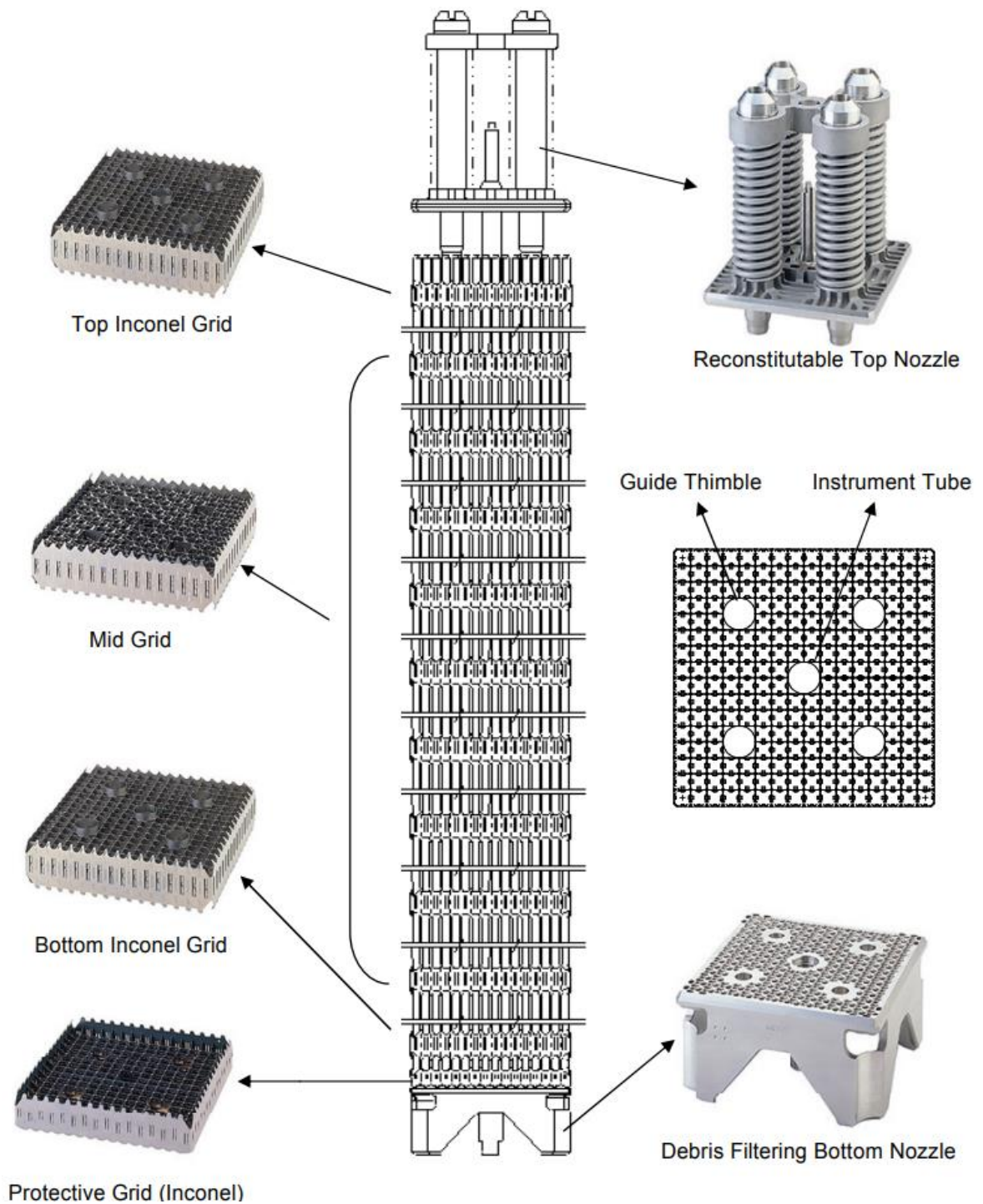
**Figure 5. PLUS7 Fuel Assembly Configuration** [4]

The top nozzle serves as an alignment and locating device for each fuel assembly and has features to permit lifting of the fuel assembly. Bottom nozzle provides the mechanical support for the fuel assembly structure. The instrument tube is inserted into sockets in the top and bottom nozzles. Each guide thimble displaces four fuel rod positions and provides channels that guide the CEAs over their entire length of travel. The nine mid-grids, one top grid and one bottom grid, and one protective grid maintain the fuel rod array by providing positive lateral restraint to the fuel rod but only friction restraint to axial fuel rod motion.

Table 4. Parameters of Fuel Assemblies and Rod [1]

| Fuel Assemblies | |
|---|---|
| Fuel rod array | Square, 16 × 16 |
| Fuel rod pitch, cm | 1.2852 |
| Weight of fuel assembly, kg | 638.9 |
| Fuel Rod | |
| Pellet material | $UO_2$ |
| Pellet diameter, cm | 0.8192 |
| Pellet length, cm | 0.98 |
| Pellet density, g/cm$^3$ | 10.44 |
| Pellet theoretical density, g/cm$^3$ | 10.96 |
| Pellet density (% T.D.) | 95.25 |
| Stack height density, g/cm3 | 10.313 |
| Clad material | ZIRLO |
| Clad inner diameter (ID), cm | 0.8357 |
| Clad outside diameter (OD), cm | 0.950 |
| Clad thickness, cm | 0.05715 |
| Diametral gap (cold), cm | 0.01651 |
| Active length, cm | 381 |
| Plenum length, cm | 25.4 |

The fuel rods consist of slightly enriched $UO_2$ cylindrical ceramic pellets and a round wire helical type 302 stainless steel compression spring, both encapsulated within a cladding and seal welded with Zircaloy-4 end caps. A schematic drawing of the fuel rod is provided in Figure 6. The cross section of the fuel assemblies is shown in Figure 7 [1].

Table 5. Parameters of Grids [1]

| | Mid-Grid | Top and Bottom Grid | Protective Grid |
|---|---|---|---|
| Type | Conformal spring | Vertical spring | Dimple |
| Material | ZIRLO | Inconel 718 | Inconel 718 |
| Number per assembly | 9 | 2 | 1 |
| Weight each, kg | 0.89 | 0.65 | 0.38 |
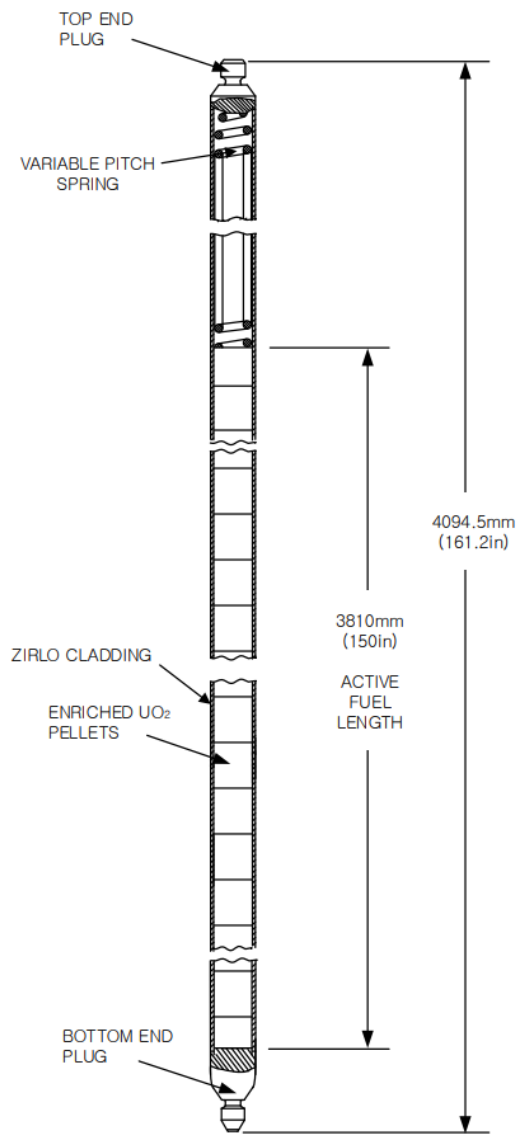
**Figure 6. Schematic Design of a Fuel Rod** [1]
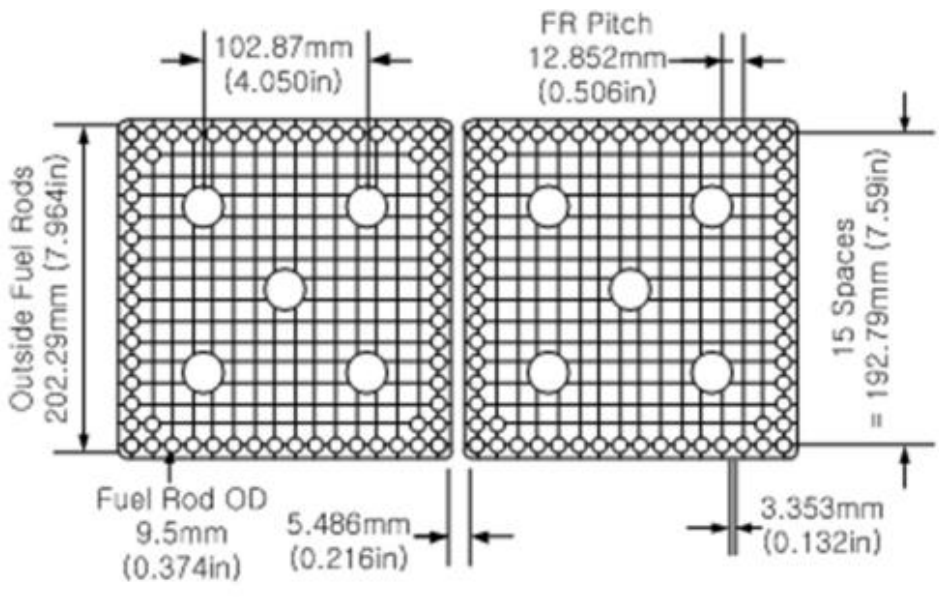


**Figure 7. Cross Section of the fuel assemblies** [1]

# 2. SUBCHANNEL ANALYSIS

In this chapter introducing the principles of subchannel analysis. The subchannel code ALTHAMC12 is considered, as well as the features of this code, such as features of entering of input parameters for calculations to the code as creating a special input generator for this.

## 2.1 Basics of methodology

Subchannel analysis is used to verify the thermal-hydraulic security characteristics of the reactor core, in particular the definition of coolant parameters in concrete place of the reactor core. The safety margins and the operating power limits of nuclear reactor core under different conditions of primary system i.e. system pressure, coolant inlet temperature, coolant flow rate and thermal power and its distributions are considered as the key parameters for subchannel analysis.

The subchannel analysis is a widely used method for predicting the distribution of temperature, pressure, and other fluid parameters in the fuel assemblies of a nuclear reactor. This technique divides the fuel assemblies into smaller channels or subchannels and then applies a set of conservation equations to each subchannel to calculate the thermal-hydraulic behavior of the coolant flowing through them.

Subchannel analysis codes model fuel assemblies with one raw of meshes per subchannel - this is shown schematically in Figure 8 [6]. In Figure 8, the principle of the subchannel analysis is depicted. The free volume of reactor core is divided into radial subchannels which are then divided into control volumes by axial division. In each control volume, the basic equations for mass, energy, and momentum conservation are solved by a subchannel code [7].
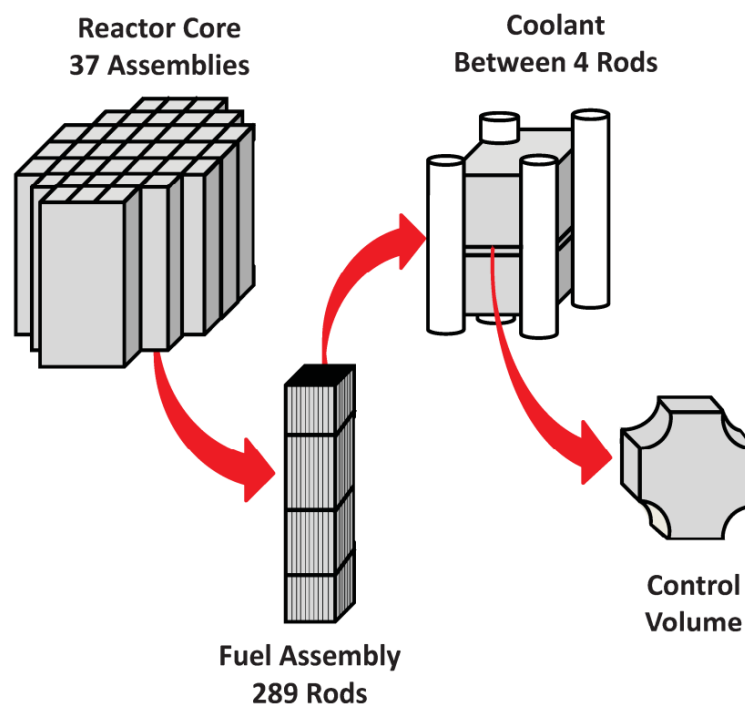


**Figure 8. Principle of subchannel analysis** [6]

A subchannel is defined as a flow passage formed between number of rods or some rods and wall of channel/shroud tube. The subchannels can be formed by either coolant centered subchannels or the rod centered subchannels as shown in Figure 9 [7].

The concept of subchannel analysis method is an important tool for predicting the thermal hydraulic performance of rod bundle nuclear fuel element. It considers a rod bundle to be a continuously interconnected set of parallel flow sub-channels which are assumed to contain one dimensional flow coupled to each other by cross flow mixing. The axial length is divided into a number of increments such that the whole flow space of a rod bundle is divided into a number of nodes.
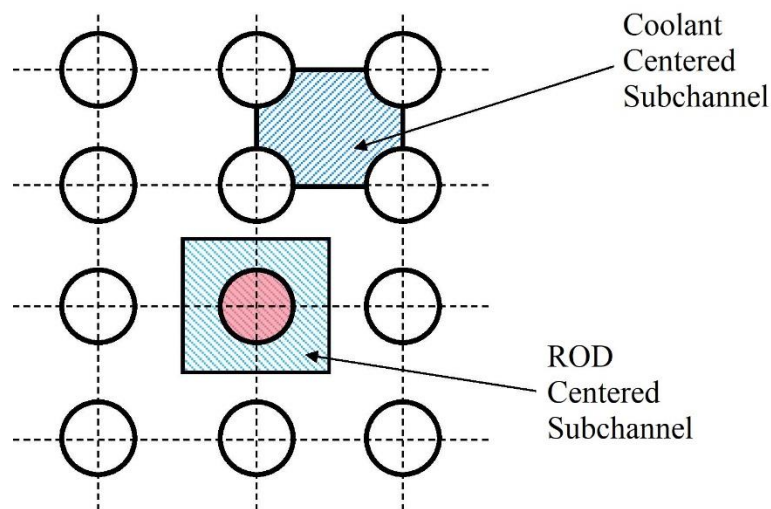


**Figure 9. Definition of fuel assembly subchannels** [7]

The subchannel analysis basically solves the conservation equations of mass, momentum and energy on the specified control volumes. A correct formulation of momentum equations and good knowledge of the mixing process between subchannels are an absolute necessity, for obtaining reliable predictions of coolant local conditions using sub-channel calculations. For more details about the subchannel analysis principles it is advised to see the references [8] and [9].

## 2.2 The ALTHAMC12 subchannel code

This chapter provides an overview of the thermalhydraulic subchannel analysis code ALTHAMC12. This subchannel code is based on the code *COBRA-IIIC* [9]. For a given core geometry and the corresponding subchannel model the code calculate the flow redistribution mode, local thermohydraulic parameters of the coolant, the temperature of the fuel rods, and the minimum margin for a boiling crisis in stationary and transient modes. The main calculation method comes from the code COBRA-IIIC.

The subchannel code utilizes several additional files with user defined names in which it is necessary to define input parameters:

1. Althamc12_module – file containing the names of the input and output files

2. TS-geom – file containing geometric characteristics and physical parameters of the model for the calculation

3. TS-regimes – file containing a set of mode parameters, which is the pressure of the coolant at the outlet to the reactor core, the flow rate of the coolant at the inlet to the reactor core (or subchannel system), temperature (or enthalpy) at the entrance to the reactor core and the total power of the reactor core (or subchannel system).

A more precise description is required for the file TS-geom. This file consists of information blocks – CARDS. In each card, which can be multiple lines, the necessary data are entered. For example: Card «SUBC» defines the basic information about the calculation - the number of modes in the TS-regimes file, or whether it is a stationary calculation or transient. In the second part, this tab allows to define the name of the calculation.

For more details about the preparation of input files it is recommended to see the reference [8].

## 2.3 Input generator in MS EXCEL for ALTHAMC12

The subchannel code ALTHAMC12 uses Fortran format. The Fortran format specification is a list of format elements describing the variable format (real number in either decimal or exponential form), the width (number of characters) of each variable, and (optionally) the number of decimal places. This format is very prone to the fact that it is extremely easy to make a mistake in the code, which, moreover, is not so easy to find. Therefore, it is recommended to create an input generator that prevents errors and monitors the writing.

To simplify the entry of input parameters for calculations, input file generator has been created for subchannel code ALTHAMC12 in MS Excel. The required data are inserted into this generator and translating in required view for the passing to the subchannel code ALTHAMC12, more specifically - to the file TS-geom. The view of this generator is shown in Figure 10.

The generator consists of three tables: Input, Output and Final. The principle of operation of the generator: all the necessary parameters are entered into the «Input» table. Data in this table is entered freely, without indents and other possible restrictions. The «Output» table is the most important in the generator. It translates data from «Input» table with the necessary indents and string lengths from each other for the code to work. And the table «Final» represents a ready-made input-deck, which will can be directly inserted into the file TS-geom.

It is very useful that the input file generator was universal for working with different types of reactors and modes. Therefore, it is advisable to leave spare rows and columns in tables.

**FINAL** | **INPUT** | **OUTPUT**

| Label | Data |
|---|---|
| *SUBC.1 | 3 \| 87 \| 1 \| 0 \| 0 |
| *SUBC.2 | Test Section 4 |
| *GEOM.1 | 36 \| 3 \| 60 \| 4 \| 25 \| 25 \| 99 \| 17 \| 3 \| 9.5 |
| *GEOM.2 | 3.658 \| 0 \| 24 |
| *GEOM.4 - subch. I | 16 \| 1 \| 87.87781 \| 29.8452 \| 29.8452 |
| *GEOM.5 | 8 \| 9 \| 10 \| 11 \| 14 \| 15 \| 16 \| 17 \| 20 \| 21 \| 22 \| 23 \| 26 \| 27 \| 28 \| 29 |
| *GEOM.4 - subch. W | 8 \| 2 \| 53.38890 \| 26.33717 \| 14.9226 |
| *GEOM.5 | 7 \| 12 \| 13 \| 18 \| 19 \| 24 \| 25 \| 30 |
| *GEOM.4 - subch. C | 4 \| 3 \| 31.982 \| 21.56127 \| 7.461275 |
| *GEOM.5 | 1 \| 6 \| 31 \| 36 |
| *GEOM.6 - junct. I-I | 24 \| 1 \| 3.1 \| 1 \| 12.6T |
| *GEOM.7 | 8 \| 8 \| 9 \| 9 \| 10 \| 10 \| 11 \| 14 \| 14 \| 15 \| 15 \| 16 \| 16 \| 17 \| 20 \| 20 |
| *GEOM.7 | 21 \| 21 \| 22 \| 22 \| 23 \| 26 \| 27 \| 28 |
| *GEOM.8 | 9 \| 14 \| 10 \| 15 \| 11 \| 16 \| 17 \| 15 \| 20 \| 16 \| 21 \| 17 \| 22 \| 23 \| 21 \| 26 |
| *GEOM.8 | 22 \| 27 \| 23 \| 28 \| 29 \| 27 \| 28 \| 29 |
| *GEOM.6 - junct. I-W | 16 \| 2 \| 3.1 \| 1 \| 10.827F |
| *GEOM.7 | 2 \| 3 \| 4 \| 5 \| 7 \| 11 \| 13 \| 17 \| 19 \| 23 \| 25 \| 29 \| 26 \| 27 \| 28 \| 29 |
| *GEOM.8 | 8 \| 9 \| 10 \| 11 \| 8 \| 12 \| 14 \| 18 \| 20 \| 24 \| 26 \| 30 \| 32 \| 33 \| 34 \| 35 |
| *GEOM.6 - junct. W-C | 8 \| 3 \| 2.3 \| 1 \| 10.661F |
| *GEOM.7 | 1 \| 1 \| 4 \| 4 \| 25 \| 31 \| 30 \| 35 |
| *GEOM.8 | 2 \| 7 \| 5 \| 12 \| 31 \| 32 \| 36 \| 36 |
| *GEOM.6 - junct. W-W | 12 \| 4 \| 2.3 \| 1 \| 12.6T |
| *GEOM.7 | 2 \| 3 \| 4 \| 7 \| 12 \| 13 \| 18 \| 19 \| 24 \| 32 \| 33 \| 34 |
| *GEOM.8 | 3 \| 4 \| 5 \| 13 \| 18 \| 19 \| 24 \| 25 \| 30 \| 33 \| 34 \| 35 |
| *RODS.1 | 1 \| 9.5 \| 0.999999 \| 0.25 \| 0.25 \| 0.25 \| 0.25 \| 0 \| 0 |
| *RODS.2 | 1 \| 0.85 \| 1 \| 2 \| 7 \| 8 |
| *RODS.1 | 1 \| 9.5 \| 0.999999 \| 0.25 \| 0.25 \| 0.25 \| 0.25 \| 0 \| 0 |
| *RODS.2 | 2 \| 0.85 \| 2 \| 3 \| 8 \| 9 |
| *RODS.1 | 1 \| 9.5 \| 0.999999 \| 0.25 \| 0.25 \| 0.25 \| 0.25 \| 0 \| 0 |
| *RODS.2 | 3 \| 0.85 \| 3 \| 4 \| 9 \| 10 |
| *RODS.1 | 1 \| 9.5 \| 0.999999 \| 0.25 \| 0.25 \| 0.25 \| 0.25 \| 0 \| 0 |
| *RODS.2 | 4 \| 0.85 \| 4 \| 5 \| 10 \| 11 |
| *RODS.1 | 1 \| 9.5 \| 0.999999 \| 0.25 \| 0.25 \| 0.25 \| 0.25 \| 0 \| 0 |
| *RODS.2 | 5 \| 0.85 \| 5 \| 6 \| 11 \| 12 |
| *RODS.1 | 1 \| 9.5 \| 0.999999 \| 0.25 \| 0.25 \| 0.25 \| 0.25 \| 0 \| 0 |
| *RODS.2 | 6 \| 0.85 \| 7 \| 8 \| 13 \| 14 |
| *RODS.1 | 1 \| 9.5 \| 0.999999 \| 0.25 \| 0.25 \| 0.25 \| 0.25 \| 0 \| 0 |
| *RODS.2 | 7 \| 1 \| 8 \| 9 \| 14 \| 15 |
| *RODS.1 | 1 \| 9.5 \| 0.999999 \| 0.25 \| 0.25 \| 0.25 \| 0.25 \| 0 \| 0 |
| *RODS.2 | 8 \| 1 \| 9 \| 10 \| 15 \| 16 |
| *RODS.1 | 1 \| 9.5 \| 0.999999 \| 0.25 \| 0.25 \| 0.25 \| 0.25 \| 0 \| 0 |
| *RODS.2 | 9 \| 1 \| 10 \| 11 \| 16 \| 17 |
| *RODS.1 | 1 \| 9.5 \| 0.999999 \| 0.25 \| 0.25 \| 0.25 \| 0.25 \| 0 \| 0 |
| *RODS.2 | 10 \| 0.85 \| 11 \| 12 \| 17 \| 18 |
| *RODS.1 | 1 \| 9.5 \| 0.999999 \| 0.25 \| 0.25 \| 0.25 \| 0.25 \| 0 \| 0 |
| *RODS.2 | 11 \| 0.85 \| 13 \| 14 \| 19 \| 20 |
| *RODS.1 | 1 \| 9.5 \| 0.999999 \| 0.25 \| 0.25 \| 0.25 \| 0.25 \| 0 \| 0 |
| *RODS.2 | 12 \| 1 \| 14 \| 15 \| 20 \| 21 |
| *RODS.1 | 1 \| 9.5 \| 0.999999 \| 0.25 \| 0.25 \| 0.25 \| 0.25 \| 0 \| 0 |
| *RODS.2 | 13 \| 1 \| 15 \| 16 \| 21 \| 22 |
| *RODS.1 | 1 \| 9.5 \| 0.999999 \| 0.25 \| 0.25 \| 0.25 \| 0.25 \| 0 \| 0 |
| *RODS.2 | 14 \| 1 \| 16 \| 17 \| 22 \| 23 |
| *RODS.1 | 1 \| 9.5 \| 0.999999 \| 0.25 \| 0.25 \| 0.25 \| 0.25 \| 0 \| 0 |
| *RODS.2 | 15 \| 0.85 \| 17 \| 18 \| 23 \| 24 |
| *RODS.1 | 1 \| 9.5 \| 0.999999 \| 0.25 \| 0.25 \| 0.25 \| 0.25 \| 0 \| 0 |
| *RODS.2 | 16 \| 0.85 \| 19 \| 20 \| 25 \| 26 |
| *RODS.1 | 1 \| 9.5 \| 0.999999 \| 0.25 \| 0.25 \| 0.25 \| 0.25 \| 0 \| 0 |
| *RODS.2 | 17 \| 1 \| 20 \| 21 \| 26 \| 27 |
| *RODS.1 | 1 \| 9.5 \| 0.999999 \| 0.25 \| 0.25 \| 0.25 \| 0.25 \| 0 \| 0 |
| *RODS.2 | 18 \| 1 \| 21 \| 22 \| 27 \| 28 |
| *RODS.1 | 1 \| 9.5 \| 0.999999 \| 0.25 \| 0.25 \| 0.25 \| 0.25 \| 0 \| 0 |
| *RODS.2 | 19 \| 1 \| 22 \| 23 \| 28 \| 29 |
| *RODS.1 | 1 \| 9.5 \| 0.999999 \| 0.25 \| 0.25 \| 0.25 \| 0.25 \| 0 \| 0 |
| *RODS.2 | 20 \| 0.85 \| 23 \| 24 \| 29 \| 30 |
| *RODS.1 | 1 \| 9.5 \| 0.999999 \| 0.25 \| 0.25 \| 0.25 \| 0.25 \| 0 \| 0 |
| *RODS.2 | 21 \| 0.85 \| 25 \| 26 \| 31 \| 32 |

**Figure 10. View of the input file generator**

# 3. MODEL OF APR-1400 REACTOR CORE

The chapter illustrates the step-by-step process of developing a model of the APR1400 reactor. This involves partitioning the model into subchannels, determining the geometric and physical parameters, and other relevant aspects.

## 3.1 Nodalization of the model

For the model of the APR1400 reactor, a quarter of the reactor core was selected as it is done in APR1400 Design Control Document [1]. In this model, one subchannel represents one fuel assembly, thus there is 69 subchannels. Subchannels are numbered and divided into different types as shown in Figure 11. There are 6 types that have different geometric parameters, depending on the location. Also, the figure indicates the number of subchannels of this type. For example, type "INNER" - subchannels are located inside the reactor core and do not touch the shroud, which is indicated by yellow lines in the figure. There are 41 such subchannels.

Specifically, this type of subchannel was taken as an example in the subchapters 3.2 - 3.7 for example calculation of geometric parameters of one subchannel.
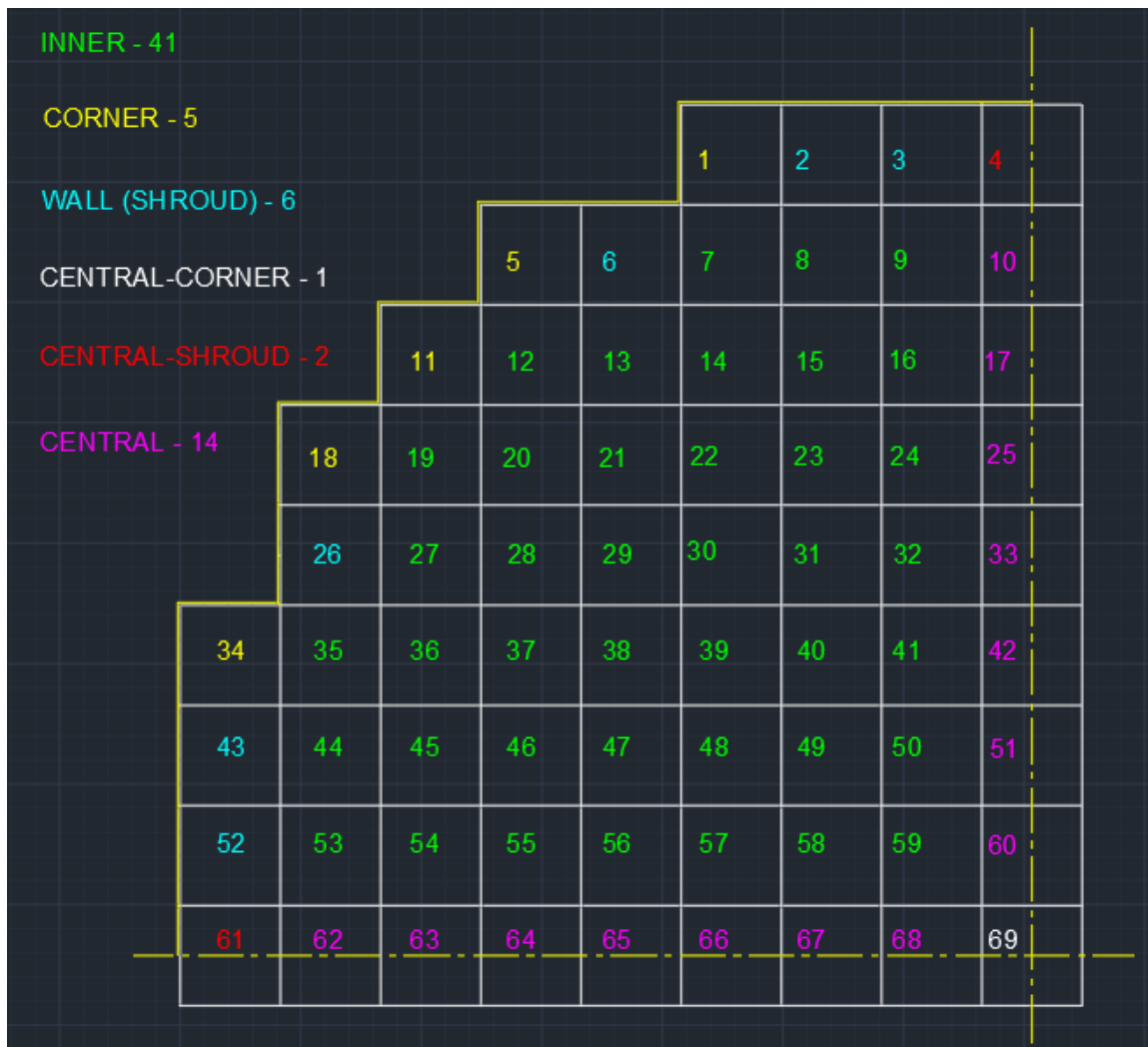


**Figure 11. Numbering of subchannels and fuel assemblies**

### 3.2 Parameters of the subchannels

In this subchapter, main parameters to the input file of the subchannel code ALTHAMC12 are specified. An example is given here for the „INNER" subchannel type, as mentioned in the previous subchapter.

Subchannel type "INNER" represents a complete fuel assembly. Its heated perimeter corresponds to the sum of the perimeters of all fuel rods in one fuel assembly.

$$P_h = P_{fr} \cdot N_{fr} = \pi \cdot d_{fr} \cdot N_{fr} = \pi \cdot 9{,}5 \cdot 236 = 7043{,}45 \ mm$$

where $P_h$ - heated perimeter [mm], $P_{fr}$ - perimeter of the fuel rod [mm], $d_{fr}$ – diameter of the fuel rod [mm], $N_{fr}$ - number of fuel rods [-]

Its wetted perimeter then corresponds to the sum of the perimeters of all fuel rods and the guide thimbles.

$$P_s = P_{fr} \cdot N_{fr} + P_{gt} \cdot N_{gt} = \pi \cdot d_{fr} \cdot N_{fr} + \pi \cdot d_{gt} \cdot N_{gt} = \pi \cdot 9{,}5 \cdot 236 + \pi \cdot 24{,}89 \cdot 5$$
$$= 7434{,}42 \ mm$$

where $P_s$ - wetted perimeter [mm], $P_{gt}$ - perimeter of the guide thimble [mm], $d_{gt}$ – diameter of the guide thimble [mm], $N_{gt}$ - number of guide thimbles [-]

The flow area $S$ is then calculated as the area of a square $S_{square}$, defined by the dimensions of the fuel assembly and half the space between fuel assemblies. In the case of the subchannel type "INNER", this type does not touch the shroud, so the shroud is not taken into account in the calculation of the area. And from the area of the square, it is necessary to subtract the area of fuel rods $S_{fr}$ and guide thimbles $S_{gt}$.

$$S = S_{square} - S_{fr} - S_{gt} = (a + x)^2 - \pi \cdot \frac{d_{fr}^2}{4} \cdot N_{fr} - \pi \cdot \frac{d_{gt}^2}{4} \cdot N_{gt}$$
$$= (202{,}29 + 5{,}486)^2 - \pi \cdot \frac{9{,}5^2}{4} \cdot 236 - \pi \cdot \frac{24{,}89^2}{4} \cdot 5 = 24009{,}85 \ mm^2$$

where $a$ - side of a square [mm], $x$ - side of a space between fuel assemblies [mm]

### 3.3 Parameters of the junctions

Regarding the junctions of subchannels, three main parameters are necessary to determine: length of the boundary, their number and distance between centers of mass of subchannels. The length of the boundary between subchannels of the "INNER" type is equal to the side of the square and the distance between fuel assemblies.

$$l = a + x = 202{,}29 + 5{,}486 = 207{,}77 \ mm$$

where $l$ - length of the boundary [mm]

Centers of mass of subchannels and the distance were found using AutoCAD [15]. Subchannel type "INNER" is symmetrical and the center of mass is in the middle of the fuel assembly. The distance between the centers of mass of the subchannels type "INNER" is shown in Figure 12 and equal 207,77 mm.
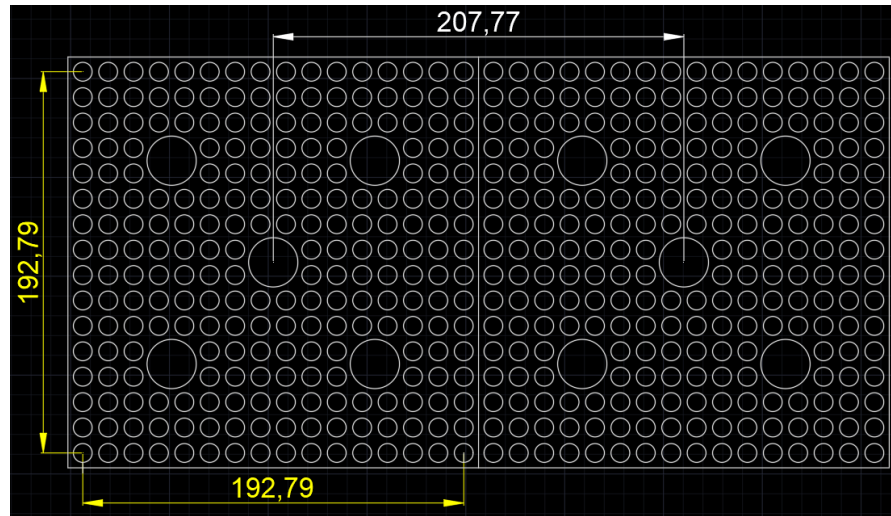


**Figure 12. Centers of mass of subchannels type "INNER"**

In the case of the subchannel type "INNER", the total number of the boundaries with other subchannels of the same type are 68 in total.

### 3.4 Parameters of the rods

Within the framework of geometry, it is also necessary to describe the fuel rods. Since a fuel assembly is accepted for one subchannel, the diameter will be the sum of the diameters of all fuel rods and thus, all fuel rods in the fuel assembly are replaced by one fictitious rod, which is wetted by only one subchannel.

$$d_{fict} = d_{fr} \cdot N_{fr} = 9,5 \cdot 236 = 2242 \, mm$$

where $d_{fict}$ - diameter of the fictitious rod [mm]

### 3.5 Radial and axial power distribution

This subchapter describes the settings for radial and axial power models to the input file of the subchannel code ALTHAMC12.

The values of the rod radial power in each fuel assembly were taken from the APR1400 Design Control Document [1] and indicated in Figure 13 (avg. rod radial power factor). Axial power values were found using the graph shown in Figure 14 using the code WebPlotDigitizer [17]. This graph shows the dependence of axial power on a fraction of active core height - 21 positions are accepted as input design parameters, the axial length and power are indicated for each position.

| | | | | | | | | |
|---|---|---|---|---|---|---|---|---|
| **ASSY AVG. ROD RADIAL POWER FACTOR** **ASSY MAX. ROD RADIAL POWER FACTOR** | | | | | 0.61 / 1.01 | 0.76 / 1.06 | 0.83 / 1.12 | 0.81 / 1.07 |
| | | | 0.65 / 1.04 | 0.88 / 1.14 | 0.98 / 1.17 | 1.09 / 1.22 | 1.12 / 1.24 | 1.19 / 1.30 |
| | | 0.74 / 1.11 | 1.08 / 1.27 | 1.10 / 1.23 | 0.95 / 1.02 | 1.20 / 1.30 | 0.97 / 1.05 | 1.15 / 1.24 |
| | 0.65 / 1.04 | 1.08 / 1.27 | 1.15 / 1.24 | 0.97 / 1.05 | 1.14 / 1.22 | 0.96 / 1.03 | 1.12 / 1.20 | 0.94 / 1.01 |
| | 0.88 / 1.14 | 1.10 / 1.22 | 0.97 / 1.05 | 1.22 / 1.31 | 0.97 / 1.04 | 1.19 / 1.28 | 0.95 / 1.02 | 1.11 / 1.18 |
| 0.61 / 1.01 | 0.98 / 1.17 | 0.95 / 1.03 | 1.14 / 1.22 | 0.97 / 1.04 | 1.15 / 1.22 | 0.97 / 1.04 | 1.13 / 1.21 | 0.95 / 1.02 |
| 0.76 / 1.06 | 1.09 / 1.22 | 1.20 / 1.29 | 0.96 / 1.03 | 1.19 / 1.27 | 0.97 / 1.03 | 1.21 / 1.29 | 0.97 / 1.03 | 1.19 / 1.27 |
| 0.83 / 1.13 | 1.12 / 1.24 | 0.97 / 1.05 | 1.12 / 1.20 | 0.95 / 1.02 | 1.13 / 1.21 | 0.97 / 1.03 | 1.13 / 1.21 | 0.93 / 1.01 |
| 0.81 / 1.08 | 1.19 / 1.30 | 1.15 / 1.25 | 0.94 / 1.01 | 1.11 / 1.18 | 0.95 / 1.02 | 1.19 / 1.27 | 0.93 / 1.01 | 0.90 / 0.95 |

**Figure 13. Core-Wide Planar Power Distribution**

## 3.6 Parameters of the grids

The subchannel code ALTHAMC12 allows to enter different types of grids. PLUS7 fuel assembly has mixing vanes and non-mixing vanes grids. It is necessary to determine the axial position in which the grid is located and to define the hydraulic resistance of the grid in the axial position. The axial positions are taken over from the Critical Heat Flux Correlation for PLUS7 Thermal Design report [10], and are shown in Figure 15. The hydraulic resistance was chosen according to the PSBT benchmark as recommended by supervisor [12].
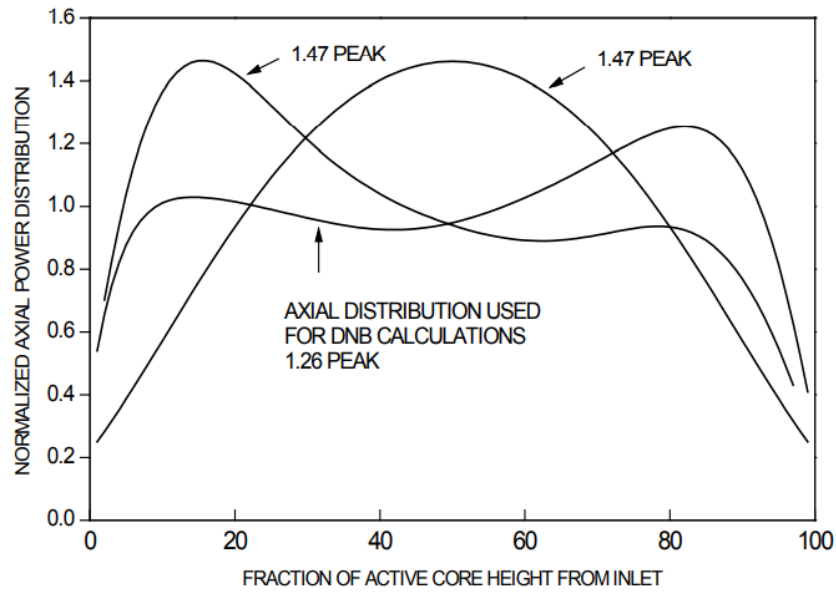
**Figure 14. Axial Power Distribution**

It should be noted that it is necessary to take into account only those grids that are in the heating zone. Figure 15 shows that there are 10 such grids, 9 of which are mixing vane and 1 non-mixing vane.
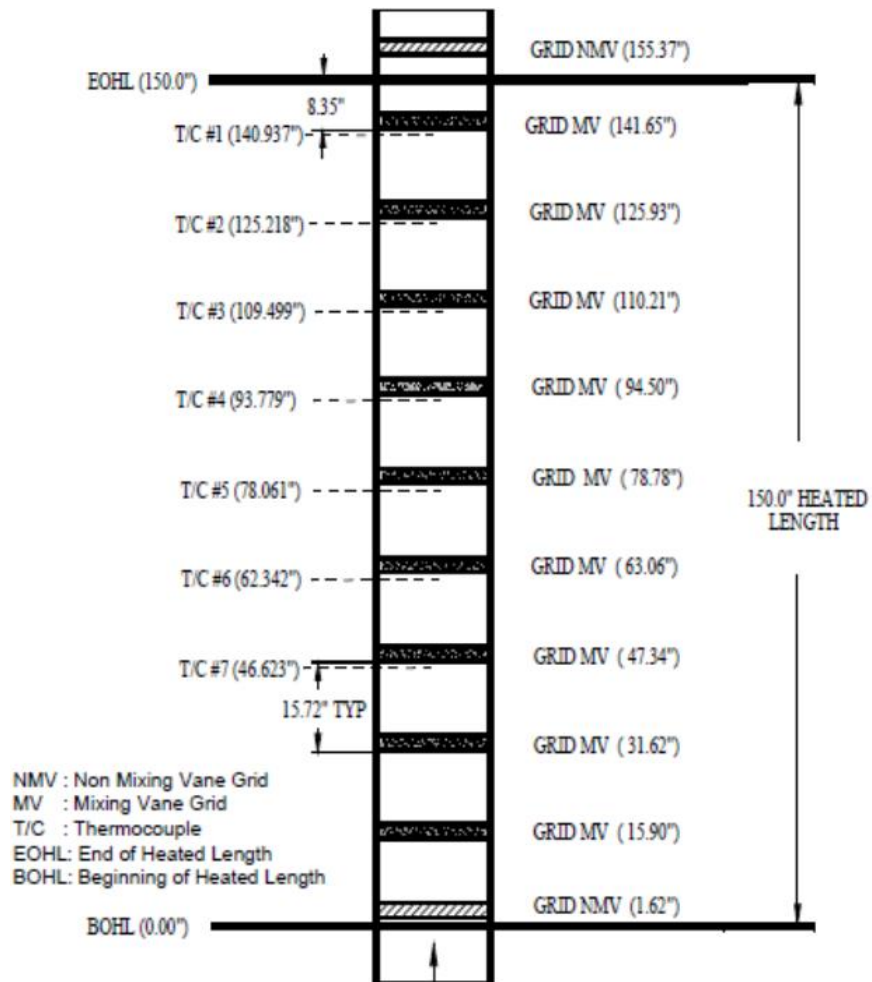


**Figure 15. Axial Configuration of the fuel rod**

### 3.7 Parameters of the coolant flow

Subsequently, it is necessary to define the turbulent mixing coefficient in the input file. The value of this coefficient is taken over from reference [11]. Because the fuel value is accepted for one subchannel and the distance between fuel rods is considered as the distance between subchannels, this coefficient must be adjusted. The value of this coefficient:

$$\beta = \frac{\beta_0}{n} = \frac{0{,}038}{16} = 0{,}00237$$

where $\beta_0$ - turbulent mixing parameter for single-phase [-], $n$ - number of rows of fuel rods in the fuel assembly [-]

After correction, this coefficient approaches zero and is practically not taken into account in the calculations.

At the next stage, it is necessary to determine the model of the hydraulic resistance of the cross-flow, which is defined in the subchannel code ALTHAMC12 by equation:

$$f = ABETA \cdot Re^{BBETA} + CBETA$$

where $f$ - model of the hydraulic resistance of the cross-flow [-]

The value of these coefficients was calculated using Idelchik's hydraulic resistance reference book [12]. According to the reference book, the coefficient BBETA for a bundle of smooth tubes with in-line arrangement, which is the fuel assembly of the APR1400 reactor, is equal $BBETA = -0{,}2$. This model does not take into account additional losses due to temperature differences at the inlet and outlet, so the coefficient $CBETA = 0$. Coefficient ABETA is found by equation:

$$ABETA = 1{,}8 \cdot \left(\frac{l_{fr}}{d_{fr}} - 1\right)^{-0{,}5} \cdot n = 1{,}8 \cdot \left(\frac{12{,}852}{9{,}5} - 1\right)^{-0{,}5} \cdot 16 = 48{,}484$$

where $l_{fr}$ – distance between fuel rods [mm], $d_{fr}$ – diameter of the fuel rod [mm], $n$ - number of rows of fuel rods in the fuel assembly [-]

# 4. VALIDATION OF THE MODEL OF APR1400 REACTOR CORE

This chapter presents the procedural guidelines for verifying and validating plant models, using the example of the APR1400 reactor model to demonstrate the validation process of the subchannel analysis code ALTHAMC12.

## 4.1 Verification and validation

Verification and validation are activities aimed at controlling the quality of the model and detecting errors in it. Having a common goal, they differ in the sources of properties, rules and restrictions that are checked during their course, the violation of which is considered an error.

Verification is a confirmation that the terms of reference were completed correctly. Validation is checking that the final product functions as it was expected from it. It may happen that the technical specification is completed correctly, but the final product works in a completely different way than expected from it. Therefore, validation is a more revealing and comprehensive concept than verification.

## 4.2 Procedure of verification and validation of plant model

Performing V&V of a plant model is a complex task that is performed in several steps. A general flow chart illustrating this procedure is shown in Figure 16. The main activities are briefly summarized below. The Figure 16 together with description of the steps is adopted from reference [13].

Prior to commencing a verification and validation process, it is essential to establish a clear specification for the plant model that will be analyzed. This represents the initial step, which involves defining the facility and objectives of the analysis. Subsequently, the process branches out into several stages, some of which can be executed concurrently.

On the right side of the figure, there are Selection of the approach and Selection of a computer code tasks. The chosen approach is largely contingent on national regulatory prerequisites and must be established or consented upon with the end-user of the analysis results. This approach should explicitly specify the types of computer codes that are acceptable for the verification and validation of the plant model. Moreover, these codes should be globally recognized and of high rate. Validation of codes is a prerequisite for their selection, and this procedure is to be done with subchannel analysis code ALTHAMC12.
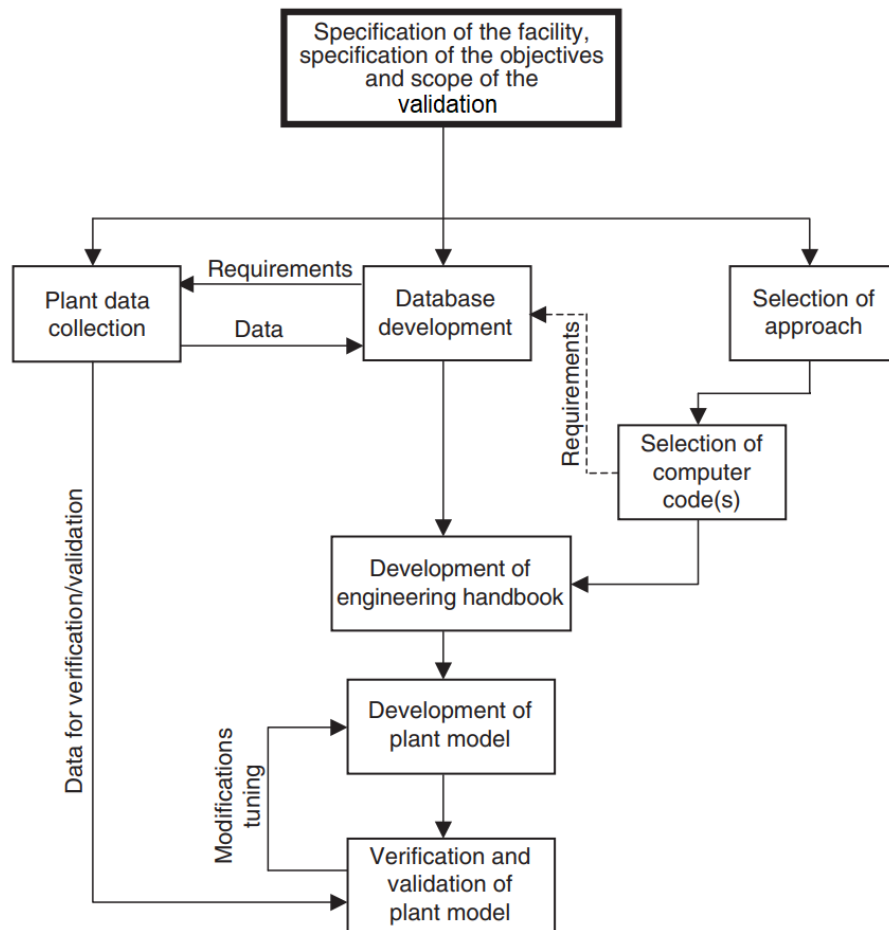
**Figure 16. Procedure of verification and validation of the plant model**

On the left side of the figure there is Plant data collection. As designed documentation or as built documentation as well as operational documentation of the plant model needs to be collected, checked and referenced. This information is essential in creating the database.

Another step is Database for the V&V. The plant model should be prepared using dependable plant data. The reason for the database development for the V&V of the plant model is to collect, formalize and reference in appropriate form all the data.

The next step is Development of engineering handbook. This document should provide a complete description of how the plant data was converted into an input data file for the computer code. Based on the engineering handbook, it is necessary to develop an input data file representing a reference plant. Plant model may include data describing the geometry, material properties, flow regimes, core kinetics, plant controllers and safety systems.

The last step is Verification and validation of the plant model. The input data must be verified and validated to ensure that the requirements of the simulation are fully met and that the performance and functionality of the input file is adequate.

**4.3 Validation of the APR1400 core model against published data**

The validation process involves comparing the results obtained from the APR1400 core model to the published data. The subchapter will also provide a summary of the published data that was used for the validation.

The APR1400 core model is a mathematical and physical simulation of a nuclear reactor core. The model is developed based on various parameters such as fuel assembly geometry, reactor coolant flow rate, thermal power and its distributions. The model's accuracy and reliability can only be determined through a rigorous validation process, which involves comparing the results obtained from the model with data published in the literature.

The subchapter discusses any discrepancies or differences observed between the model and the published data, and describe any efforts made to address these differences.

**4.3.1 Validation against core general parameters at steady state**

The APR1400 core model, created using the subchannel analysis code TORC, was taken as the reference data for validation [1]. TORC is a subchannel analysis code used in the field of nuclear engineering to simulate the thermal-hydraulic behavior of fuel assemblies in nuclear reactors. The code is developed by Korea Atomic Energy Research Institute (KAERI) and is widely used in the nuclear power industry for analyzing the performance of pressurized water reactors (PWRs). As well as subchannel analysis code ALTHAMC12, The TORC code is based on the code COBRA IIIC. The difference between reference data for full reactor power and received data are indicated in Table 6 [1].

Table 6. Comparison of the core general parameters at steady state

| Reactor Parameter | Reference data [1] | Received data | Difference [%] |
|---|---|---|---|
| Primary system pressure [MPa] | 15.51 | 15.51 | - |
| Reactor inlet coolant temperature [°C] | 290.6 | 290.6 | - |
| Core flow [kg/sec] | 4914.9 | 4914.9 | - |
| Core power level, MWt | 995.75 | 995.75 | - |
| Reactor outlet coolant temperature [°C] | 325 | 325.99 | 0.30 |
| Average coolant temperature rise [°C] | 34.4 | 35.39 | 2.88 |
| Core average fuel rod heat flux [MW/m$^2$] | 0.601 | 0.64 | 6.49 |
| Average exit equilibrium quality fraction | -0.145 | -0.143 | 1.39 |
| Inlet Average coolant density [kg/m$^3$] | 744.9 | 745.084 | 0.02 |
| Outlet Average coolant density [kg/m$^3$] | 669.6 | 662.828 | 1.02 |
| Average coolant enthalpy rise [kJ/kg] | 195.39 | 204.42 | 4.62 |

In Table 6, green color indicates input parameters such as pressure, inlet temperature and core flow which are the same for both models. The blue color indicates the parameters obtained from the subchannel analysis. Results showed that the reactor parameters obtained were very similar, with a difference that did not exceed a few percent. Despite such a similarity of parameters between

the two codes, it cannot be said with certainty that the core model turned out to be ideal, because the 6 percent discrepancy in the core average fuel rod heat flux is not so insignificant.

The accuracy of the model, shown by the similarity between the results obtained with ALTHAMC12 and TORC, also confirms the fact that both codes use similar physical and mathematical models to model the behavior of the reactor core.

Anyway, this is a basic model, its further improvement is described in the subchapter 4.3.2.

### 4.3.2 Validation against coolant outlet properties

#### 4.3.2.1 Results of basic model

The basic model does not take into account the flow distribution in the core. More precisely, this is a simplified model in which the flow is distributed evenly over each fuel rod.

The next step is to compare the obtained results of exit equilibrium quality fraction from subchannel analysis code ALTHAMC12 against published data. The values of the exit equilibrium quality fraction were also taken from the APR1400 Design Control Document [1] and indicated in Figure 17. These parameters are given in relative values and the difference with the reference data is calculated by the formula:

$$q_{diff} = \frac{q_{ref} - q_m}{q_{ref}}$$

where $q_{diff}$ – difference of the quality fraction [-], $q_{ref}$ – quality fraction from DCD documentation [-], $q_m$ – quality fraction of the model [-]

**EXIT VOID FRACTION**
**EXIT EQUILIBRIUM QUALITY FRACTION**

| | | | | | | | | |
|---|---|---|---|---|---|---|---|---|
| | | | | | 0.00 -0.23 | 0.00 -0.20 | 0.00 -0.18 | 0.00 -0.19 |
| | | | 0.00 -0.23 | 0.00 -0.18 | 0.00 -0.15 | 0.00 -0.12 | 0.00 -0.03 | 0.00 -0.10 |
| | | 0.00 -0.21 | 0.00 -0.13 | 0.00 -0.13 | 0.00 -0.16 | 0.00 -0.11 | 0.00 -0.15 | 0.00 -0.12 |
| | 0.00 -0.23 | 0.00 -0.13 | 0.00 -0.11 | 0.00 -0.15 | 0.00 -0.12 | 0.00 -0.15 | 0.00 -0.12 | 0.00 -0.16 |
| | 0.00 -0.17 | 0.00 -0.13 | 0.00 -0.15 | 0.00 -0.10 | 0.00 -0.15 | 0.00 -0.11 | 0.00 -0.16 | 0.00 -0.12 |
| 0.00 -0.23 | 0.00 -0.15 | 0.00 -0.16 | 0.00 -0.12 | 0.00 -0.15 | 0.00 -0.12 | 0.00 -0.15 | 0.00 -0.12 | 0.00 -0.16 |
| 0.00 -0.20 | 0.00 -0.13 | 0.00 -0.11 | 0.00 -0.15 | 0.00 -0.11 | 0.00 -0.15 | 0.00 -0.10 | 0.00 -0.15 | 0.00 -0.11 |
| 0.00 -0.18 | 0.00 -0.12 | 0.00 -0.15 | 0.00 -0.12 | 0.00 -0.16 | 0.00 -0.12 | 0.00 -0.15 | 0.00 -0.12 | 0.00 -0.16 |
| 0.00 -0.19 | 0.00 -0.11 | 0.00 -0.11 | 0.00 -0.16 | 0.00 -0.12 | 0.00 -0.16 | 0.00 -0.11 | 0.00 -0.16 | 0.00 -0.17 |

**Figure 17. Average Void Fractions and Qualities in Core Region** [1]

The obtained results and the relative difference with the reference data are indicated in Figures 18 and 19, respectively.

| | | | | | | | | |
|---|---|---|---|---|---|---|---|---|
| | | | | | -0.24 | -0.21 | -0.19 | -0.20 |
| | | | -0.23 | -0.18 | -0.16 | -0.13 | -0.13 | -0.11 |
| | | -0.22 | -0.14 | -0.13 | -0.16 | -0.11 | -0.15 | -0.12 |
| | -0.23 | -0.14 | -0.12 | -0.15 | -0.12 | -0.16 | -0.13 | -0.16 |
| | -0.18 | -0.13 | -0.15 | -0.11 | -0.15 | -0.11 | -0.16 | -0.13 |
| -0.24 | -0.16 | -0.16 | -0.12 | -0.15 | -0.12 | -0.15 | -0.13 | -0.16 |
| -0.21 | -0.13 | -0.11 | -0.16 | -0.11 | -0.15 | -0.11 | -0.15 | -0.11 |
| -0.19 | -0.13 | -0.15 | -0.13 | -0.16 | -0.13 | -0.15 | -0.13 | -0.16 |
| -0.20 | -0.11 | -0.12 | -0.16 | -0.13 | -0.16 | -0.11 | -0.16 | -0.17 |

**Figure 18. Exit equilibrium quality fraction of the basic model**

| MIN | -3.27 |
|---|---|
| MAX | 0.01 |
| AVG | -0.08 |

| | | | | | | | | |
|---|---|---|---|---|---|---|---|---|
| | | | | | -0.05 | -0.03 | -0.07 | -0.03 |
| | | | -0.01 | -0.02 | -0.04 | -0.12 | -3.27 | -0.14 |
| | | -0.03 | -0.06 | -0.01 | 0.01 | -0.01 | -0.03 | -0.01 |
| | -0.01 | -0.06 | -0.10 | -0.03 | -0.03 | -0.04 | -0.06 | 0.00 |
| | -0.08 | -0.01 | -0.03 | -0.07 | -0.03 | -0.03 | 0.01 | -0.08 |
| -0.05 | -0.04 | 0.01 | -0.03 | -0.03 | -0.01 | -0.03 | -0.04 | 0.01 |
| -0.03 | -0.03 | -0.01 | -0.04 | -0.03 | -0.03 | -0.09 | -0.03 | -0.03 |
| -0.07 | -0.07 | -0.03 | -0.06 | 0.01 | -0.04 | -0.03 | -0.05 | -0.02 |
| -0.03 | -0.04 | -0.10 | 0.00 | -0.08 | 0.01 | -0.03 | -0.02 | 0.00 |

**Figure 19. Difference of the quality fraction against published data**

As can be seen in Figure 19, the averages of the received data and the published data differ slightly. This indicates the accuracy of the model of the subchannel code ALTHAMC12. But there is one exception - the figure shows that the value of the quality of one fuel rod is exceptionally different from the published data. This phenomenon and the further improvement of the existing core model is described in detail in the subsection 4.3.2.2.

### 4.3.2.2 Sensitivity study on inlet flow distribution

For greater accuracy of the core model, it is necessary to take into account the uneven flow distribution. Revised Core Inlet Flow Distribution was chosen according to the Review on the Regionalization Methodology for Core Inlet Flow Distribution Map [14] as recommended by supervisor [12]. The data is valid for the System 80 reactor. The APR1400 reactor was designed based on the System 80 reactor and these data are also applicable.

Revised Core Inlet Flow Distribution are shown in Figures 20 and 21 [14]. The figures show the core inlet flow distribution values obtained by the two methods - ABB-CE's regionalization methodology and the Alternative Approach. For more details on these methodologies, it is recommended to see the reference [14]. Numbers underlined refer to In-core instrumentation (ICI) locations. These instruments are specifically designed to provide real-time data on important variables such as neutron flux, power distribution, coolant flow, and temperature distribution within the reactor core.

**Top View**     **Outlet** ↑

Inlet 1A →

|  |  |  |  |  | 1.01 | 1.01 | 1.01 | 1.01 |
|---|---|---|---|---|---|---|---|---|
|  |  |  | 0.99 | 1.01 | 0.96 | 0.89 | 0.96 | 0.96 |
|  |  | 1.01 | 0.96 | 1.08 | 1.03 | 1.08 | 1.03 | 1.08 |
|  | 1.01 | 0.89 | 0.96 | 0.89 | 1.01 | 1.01 | 1.01 | 1.01 |
|  | 1.01 | 1.08 | 0.96 | 1.08 | 0.99 | 1.01 | 0.99 | 1.01 |
| 1.01 | 0.89 | 1.08 | 0.99 | 1.01 | 1.01 | 1.01 | 1.01 | 0.99 |
| 1.01 | 0.96 | 1.03 | 1.01 | 1.01 | 0.99 | 1.01 | 1.01 | 1.01 |
| 1.01 | 0.96 | 1.08 | 0.99 | 1.01 | 1.01 | 1.01 | 0.99 | 1.01 |
| 0.99 | 0.96 | 1.03 | 1.01 | 0.99 | 1.01 | 1.01 | 1.01 | 0.99 |

270°
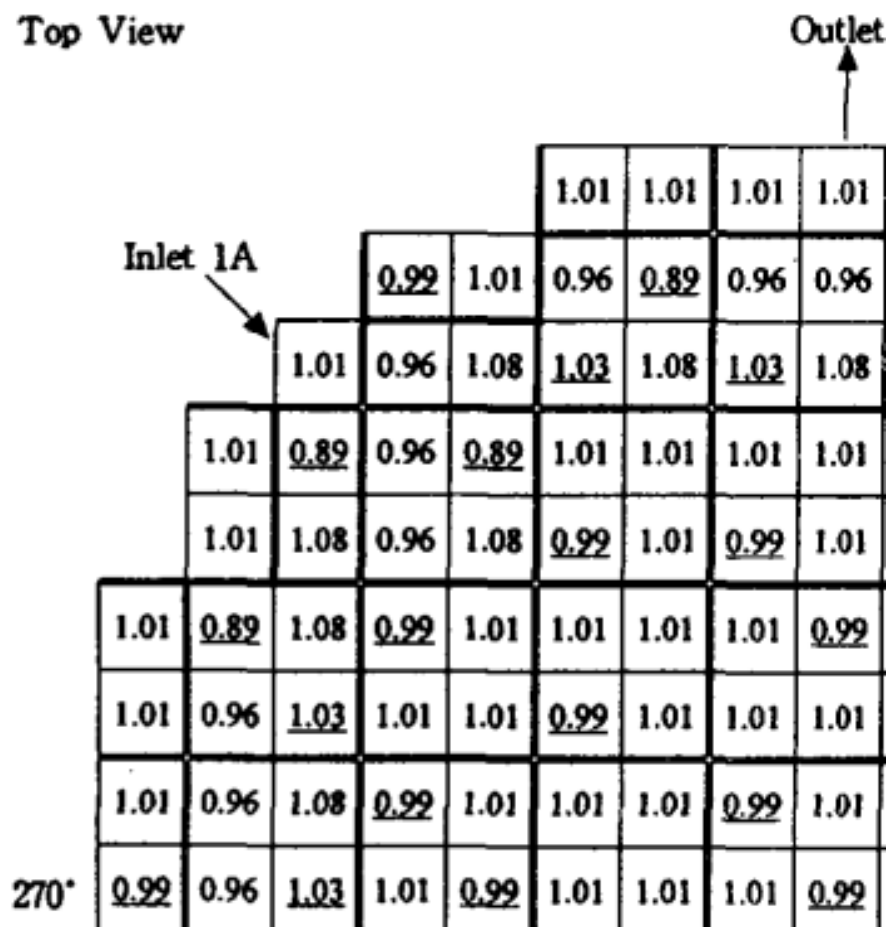
**Figure 20. Revised Core Inlet Flow Distribution by ABB-CE** [14]
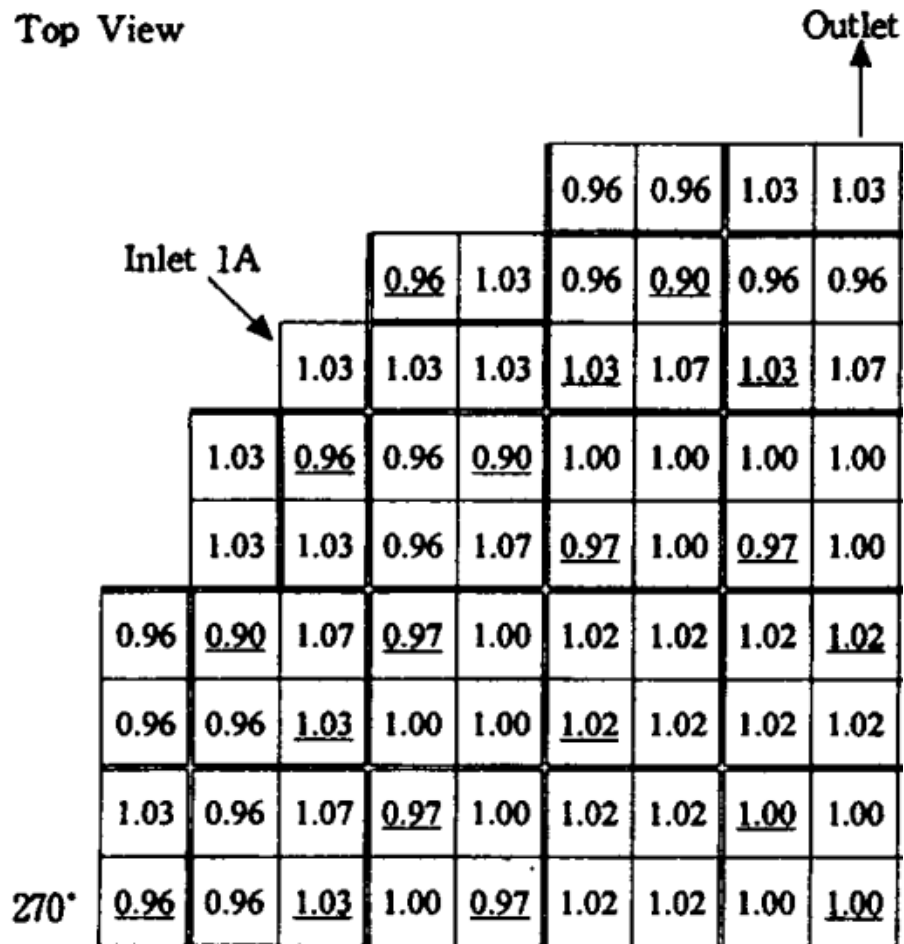
Top View

Inlet 1A

270°

**Figure 21. Revised Core Inlet Flow Distribution by the Alternative Approach** [14]

By adding data to the existing model, new values of exit equilibrium quality fraction are obtained and the relative difference with the reference data are indicated in Figures 22 and 23.

As can be seen from the figures, even with a more accurate reactor model, one fuel rod differs by an order of magnitude from the reference values of the quality. This could be due to the fact that this fuel rod is subject to detailed nodalization. But even with this nodalization, the difference is too high. So it's more likely a typo in the documentation. Figure 13 shows that the rod radial power in each fuel assembly is symmetrically distributed and there cannot be such a difference.

| MIN | -3.28 |
|-----|-------|
| MAX | 0.01 |
| AVG | -0.09 |

| | | | | | | | | |
|---|---|---|---|---|---|---|---|---|
| | | | | | -0.04 | -0.03 | -0.06 | -0.03 |
| | | | -0.01 | -0.01 | -0.04 | -0.11 | -3.28 | -0.14 |
| | | -0.02 | -0.05 | -0.01 | 0.01 | -0.02 | -0.03 | -0.01 |
| | -0.01 | -0.04 | -0.11 | -0.02 | -0.03 | -0.05 | -0.07 | -0.01 |
| | -0.07 | -0.01 | -0.02 | -0.09 | -0.03 | -0.04 | 0.00 | -0.09 |
| -0.04 | -0.03 | 0.01 | -0.03 | -0.03 | -0.02 | -0.04 | -0.06 | 0.00 |
| -0.03 | -0.03 | -0.01 | -0.05 | -0.04 | -0.04 | -0.11 | -0.04 | -0.04 |
| -0.07 | -0.07 | -0.03 | -0.07 | 0.00 | -0.06 | -0.04 | -0.05 | -0.02 |
| -0.03 | -0.03 | -0.10 | -0.01 | -0.09 | 0.00 | -0.04 | -0.02 | 0.00 |

**Figure 22. Difference of the quality fraction using ABB-CE data against published data**

| MIN | -3.24 |
|-----|-------|
| MAX | 0.02 |
| AVG | -0.09 |

| | | | | | | | | |
|---|---|---|---|---|---|---|---|---|
| | | | | | -0.04 | -0.02 | -0.06 | -0.02 |
| | | | -0.01 | -0.01 | -0.03 | -0.10 | -3.24 | -0.13 |
| | | -0.03 | -0.07 | -0.01 | 0.02 | -0.01 | -0.03 | -0.01 |
| | -0.01 | -0.07 | -0.11 | -0.03 | -0.03 | -0.04 | -0.07 | -0.01 |
| | -0.08 | -0.01 | -0.03 | -0.10 | -0.03 | -0.05 | 0.00 | -0.10 |
| -0.03 | -0.03 | 0.01 | -0.03 | -0.03 | -0.02 | -0.04 | -0.06 | 0.00 |
| -0.02 | -0.01 | -0.01 | -0.05 | -0.04 | -0.04 | -0.11 | -0.05 | -0.05 |
| -0.06 | -0.05 | -0.03 | -0.07 | 0.00 | -0.06 | -0.05 | -0.07 | -0.03 |
| -0.02 | -0.02 | -0.09 | -0.01 | -0.09 | 0.00 | -0.05 | -0.03 | -0.01 |

**Figure 23. Difference of the quality fraction using the Alternative Approach data against published data**

### 4.3.3 Validation against results accident analysis in DCD documentation

This subsection describes the analyses that have been performed for events that could result in a decrease in the reactor coolant system (RCS) flow rate [16].

The Loss of Flow Accident (LOFA) is a type of accident that can occur in pressurized water reactors (PWRs) when there is a significant reduction in the flow of coolant through the reactor core. This can lead to a reduction in the cooling capacity of the reactor, which can cause the fuel cladding to overheat and possibly rupture, releasing radioactive material into the reactor coolant.

Using the subchannel analysis code ALHTHAMC12 code, a model of the reactor core was created, in which there was the complete loss of forced reactor coolant flow results from the simultaneous loss of electrical power to all reactor coolant pumps (RCPs).

The data for comparison were taken from APR1400 Design Control Document Tier 2 – Transient and Accident Analyses [16]. In this literature, the nuclear steam supply system (NSSS) response to a complete loss of reactor coolant flow is simulated using the CESEC-III subchannel analysis code. Assumptions and initial conditions for the Loss of Forced Reactor Coolant Flow are indicated in Table 7 [16]. Changes in core flow and pressure during an accident are shown in Figures 24 and 25 respectively. How the reactor coolant temperatures change over time is shown in Figure 26.
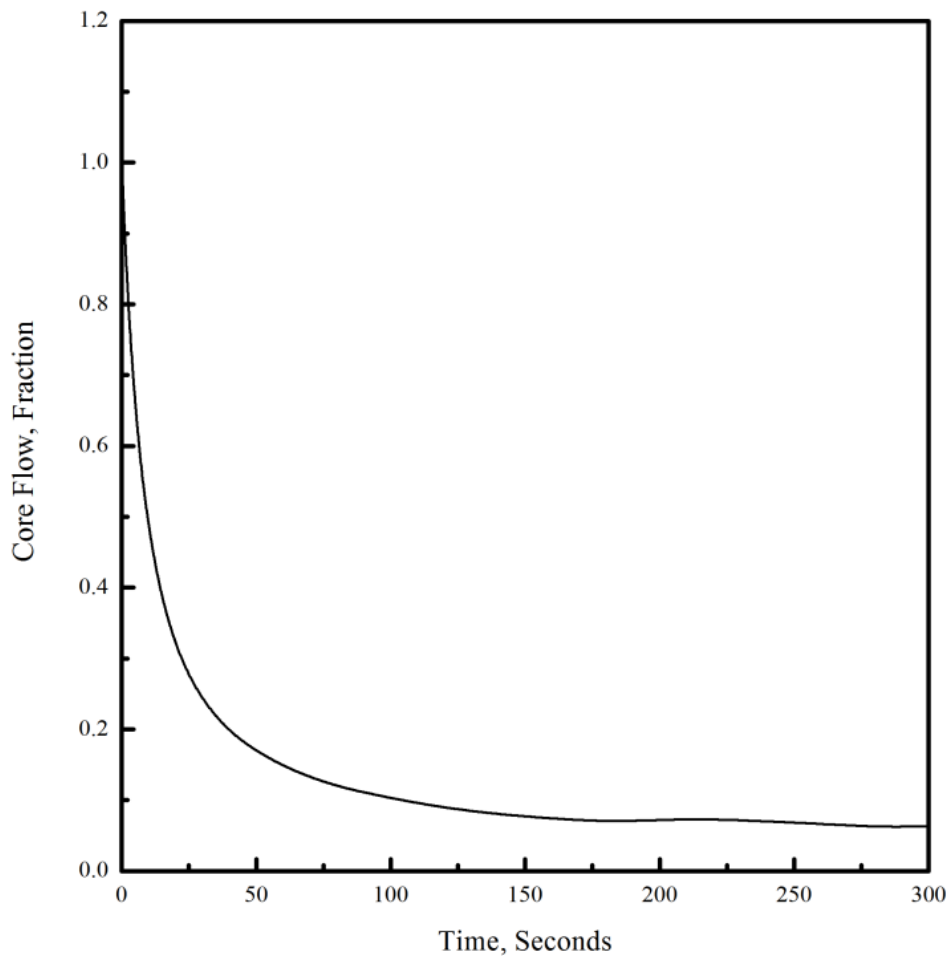


**Figure 24. Core Flow vs. Time** [16]
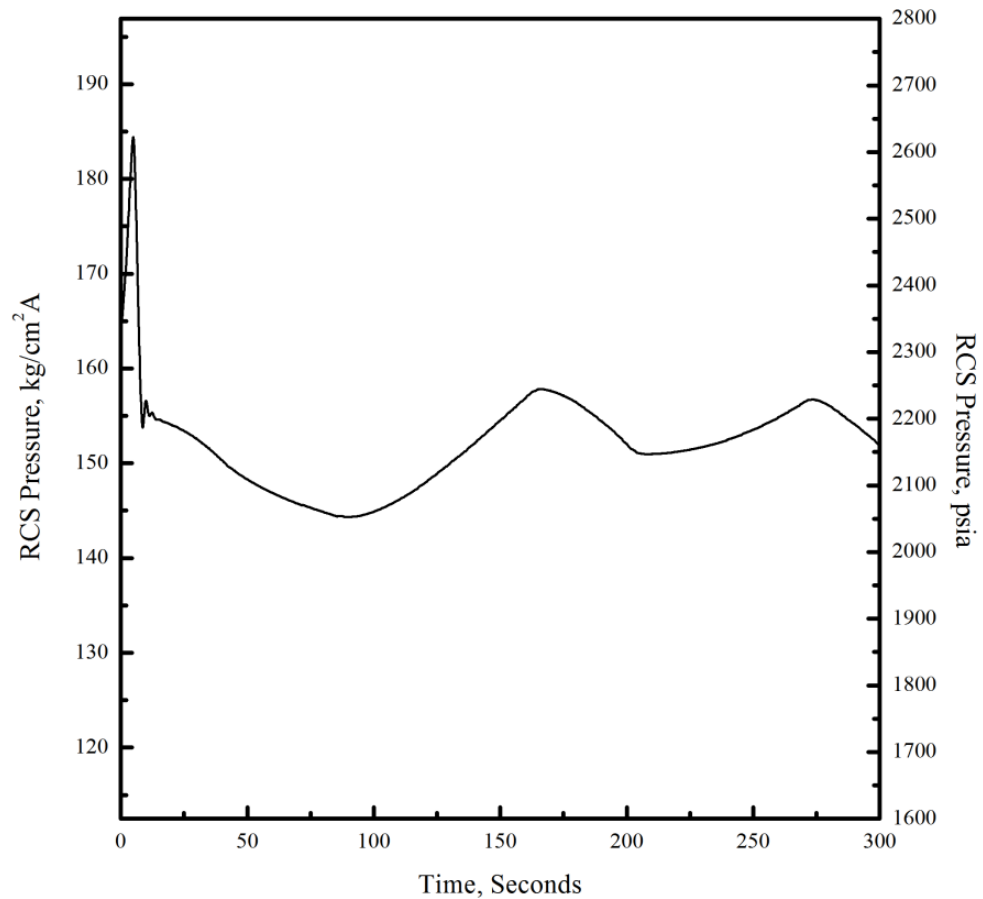
**Figure 25. RCS Pressure vs. Time** [16]

Table 7. Assumptions and initial conditions for the Loss of Forced Reactor Coolant Flow

| | |
|---|---|
| Core power level, MWt | 1015.66 |
| Core inlet coolant temperature, °C | 287.8 |
| Reactor coolant system pressure, MPa | 16.07 |
| Core mass flow, kg/s | 5904.8 |

Reactor inlet coolant temperature values were found using the graph shown in Figure 26 as well as the values of pressure, power and core flow using the code WebPlotDigitizer [17]. As input design parameters, there are 15 acceptable time intervals, and for each interval, the aforementioned parameters are specified. Obtained values of the reactor outlet coolant temperature also comparison with reference values are shown in Figure 27.

Reactor outlet coolant temperature calculated using subchannel analysis code ALTHAMC12 turned out to be close to the reference values. There is a slight deviation of the graph curve associated with the measurement error of finding the parameter values, but it is insignificant and does not exceed 1-2 percent.
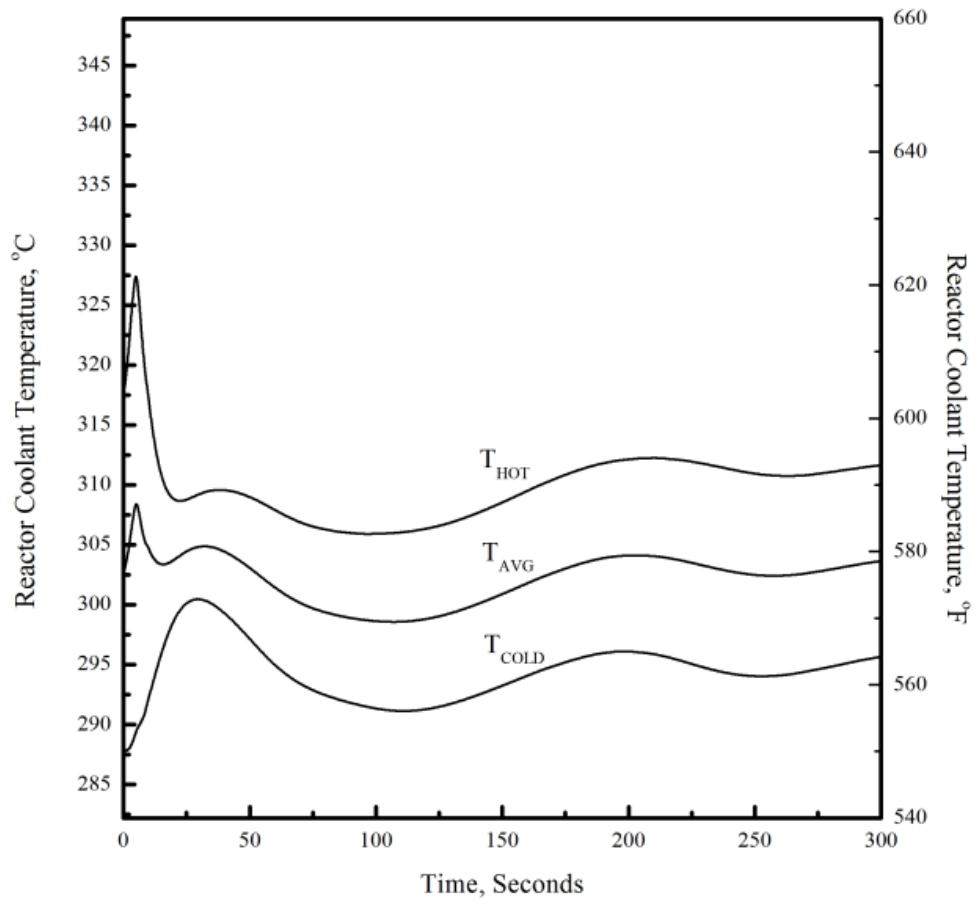
**Figure 26. Reactor Coolant Temperature vs. Time** [16]
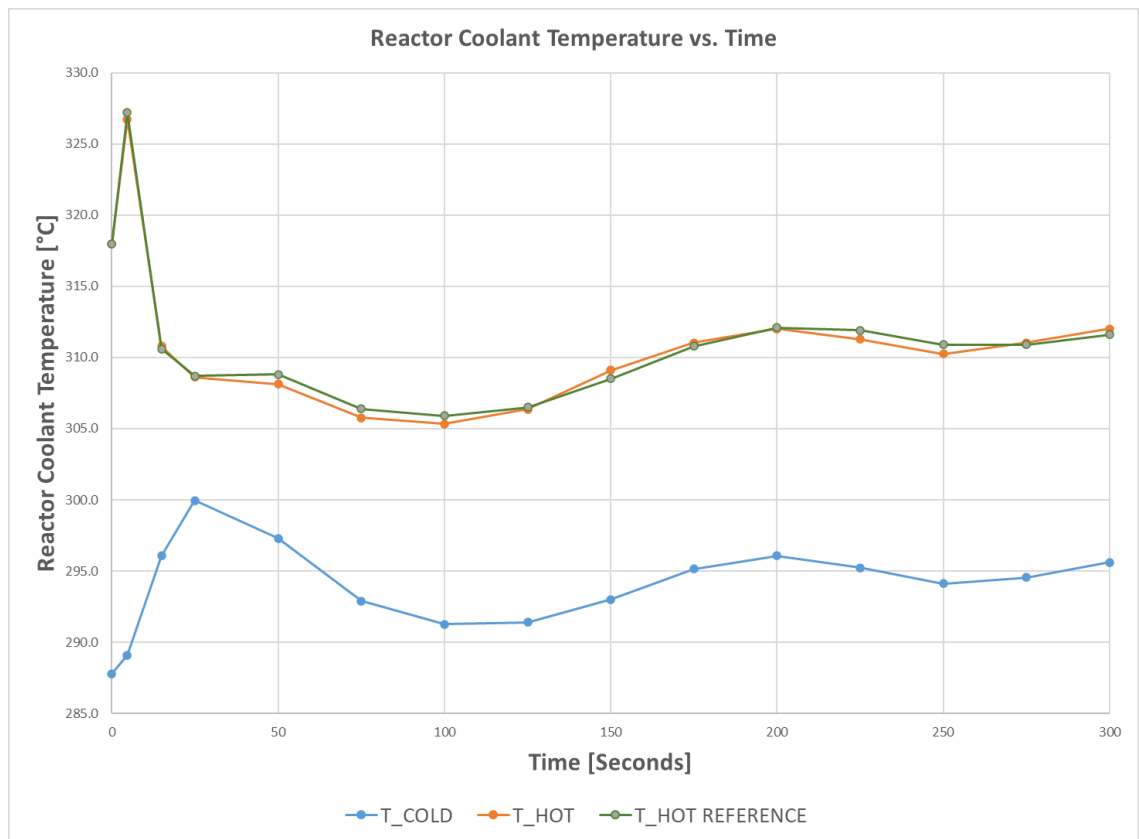


**Figure 27. Comparison of the outlet Reactor Coolant Temperature**

## 4.4 Validation against results of accident analysis from TRACE calculation

This subsection describes the analysis of an accident in which the rotor of the reactor coolant pump seizes.

The seizure of the rotor disrupts its intended rotary motion, resulting in the cessation of the coolant circulation process. Without the circulation of coolant, the reactor core's temperature can rapidly increase, potentially jeopardizing its integrity and safety.

The data for comparison were taken from the company TES s.r.o. [18]. In this model, the TRACE code was used. The analysis code TRACE serves as the authoritative thermal-hydraulic system code for Light Water Reactors (LWR) under the U.S. Nuclear Regulatory Commission (NRC). It is widely recognized as the reference best-estimate code for assessing the thermal-hydraulic behavior of these reactors. For more details about the subchannel analysis code TRACE it is advised to see the reference [19].

The nodalization of the reactor core from the analysis code TRACE, as depicted in Figure 28, shows significant differences against the model from the subchannel analysis code ALTHAMC12. The reactor is divided into 12 sections, where each channel consists of one section.
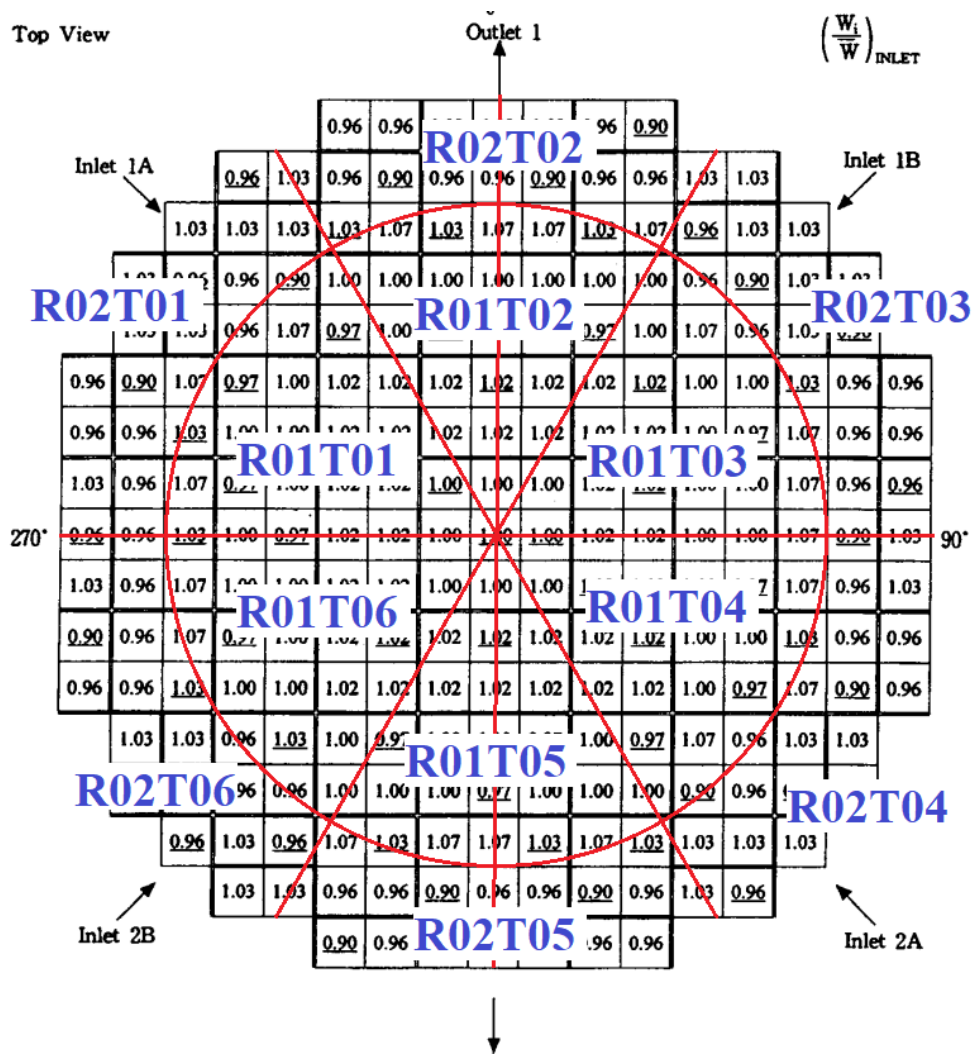


**Figure 28. Numbering of sections from TRACE calculation**

The model describes the situation when one of the reactor coolant pumps breaks down, specifically pump no. 2B (from the "Inlet 2B" side in Figure 28) For each section, the coolant parameters, flow rate, pressure and power are calculated by TES s.r.o using the subchannel analysis code TRACE. The values of the core inlet temperature in each section are shown in Figure 29 and 30.
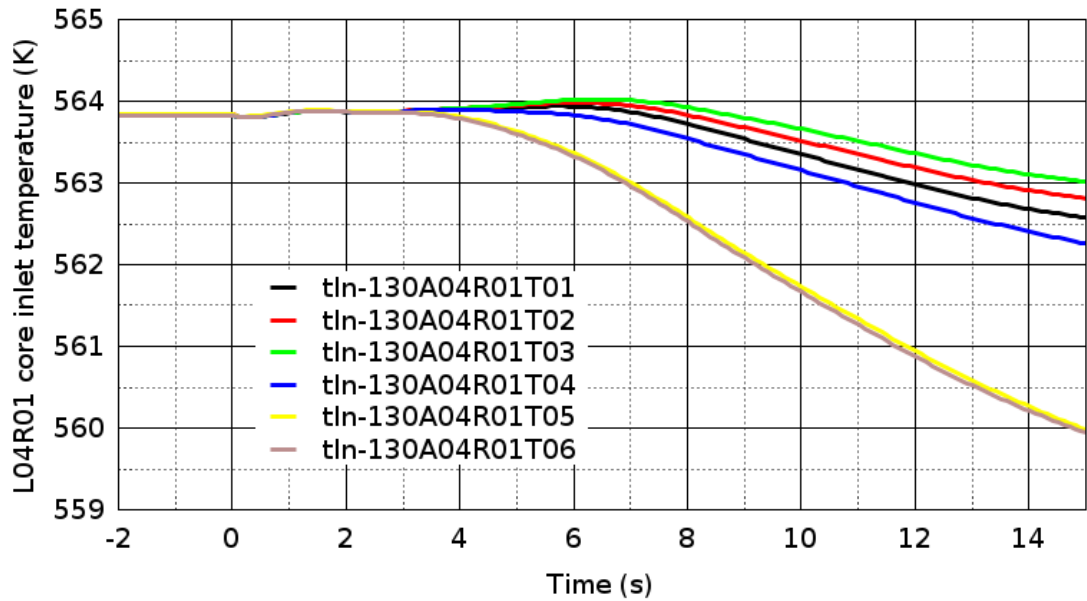


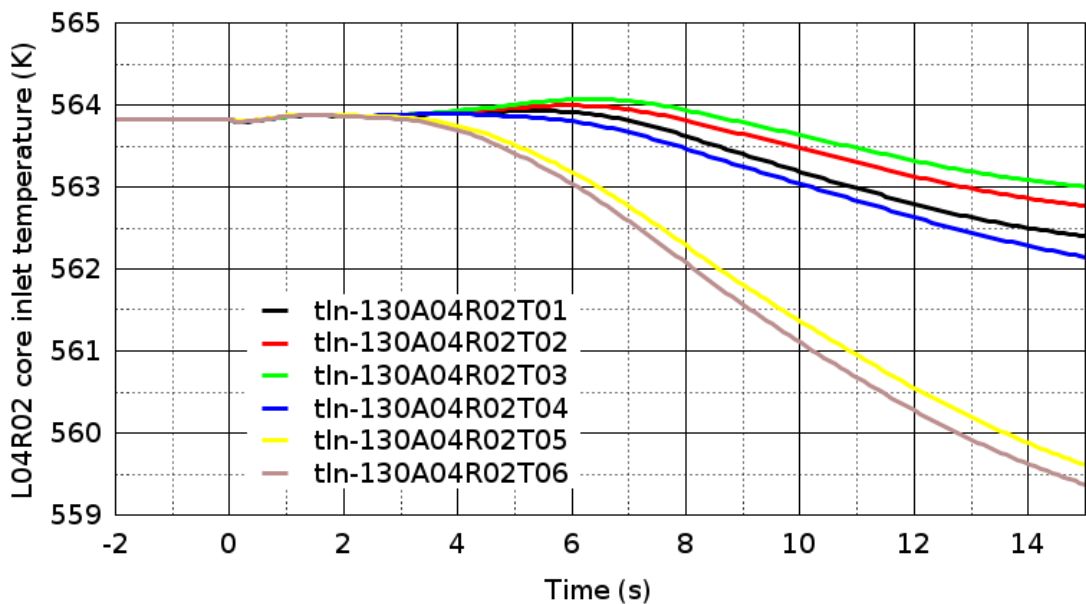**Figure 29. Core inlet temperature in sections R01**



**Figure 30. Core inlet temperature in sections R02**

For comparison, sections R01T05-06 and R02T05-06 will be considered, since they are located on the side of the seizures pump and Figures 29-30 shows that the coolant temperature drops the most there.

The core inlet pressure in each section is shown in Figures 31 and 32. And the core inlet flow rate in each section is shown in Figures 33 and 34.
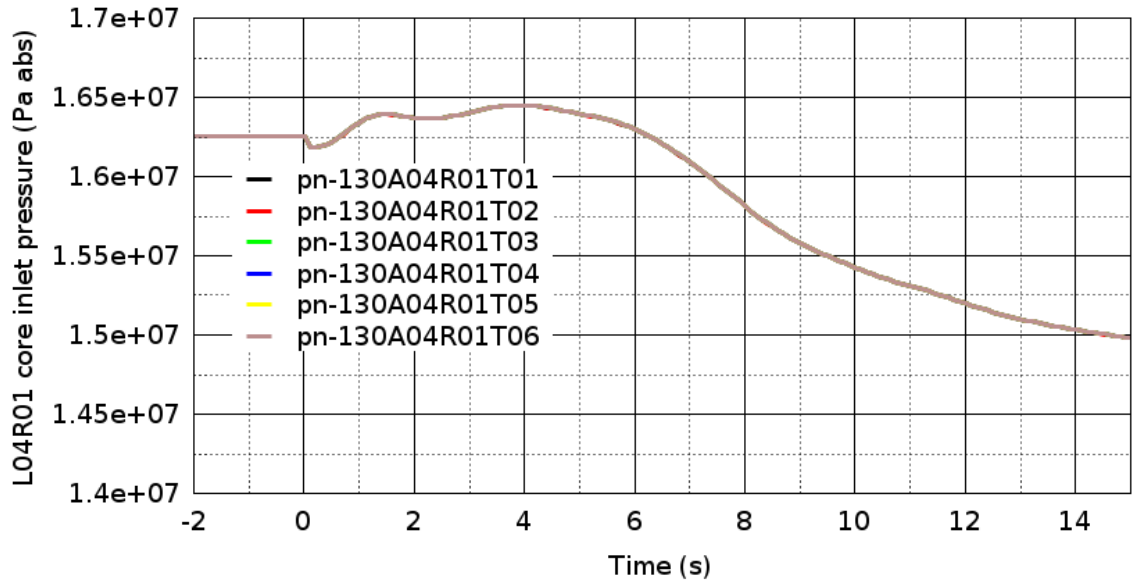


**Figure 31. Core inlet pressure in sections R01**
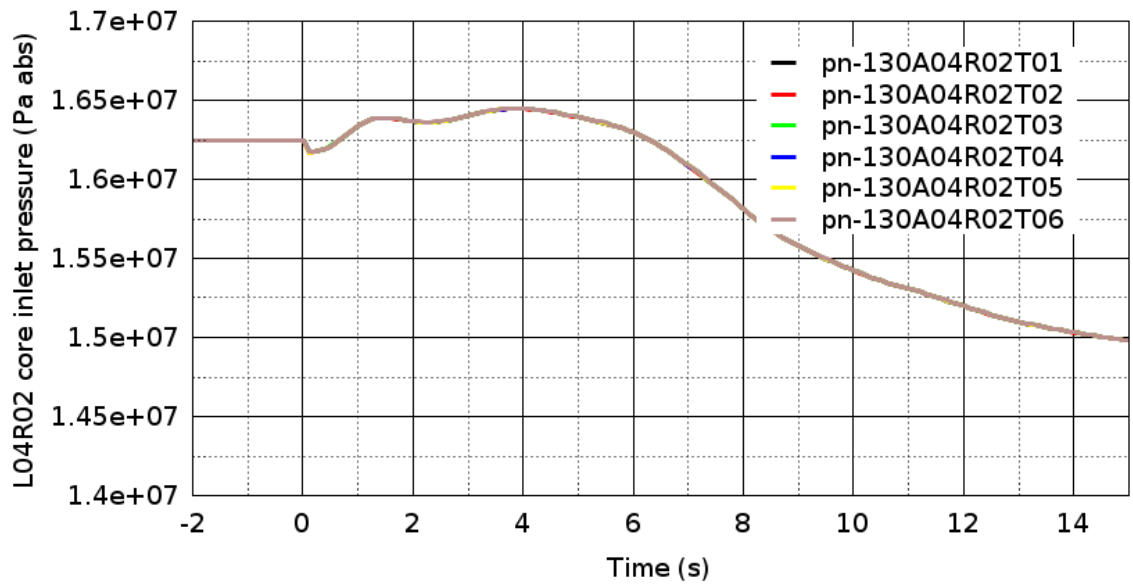


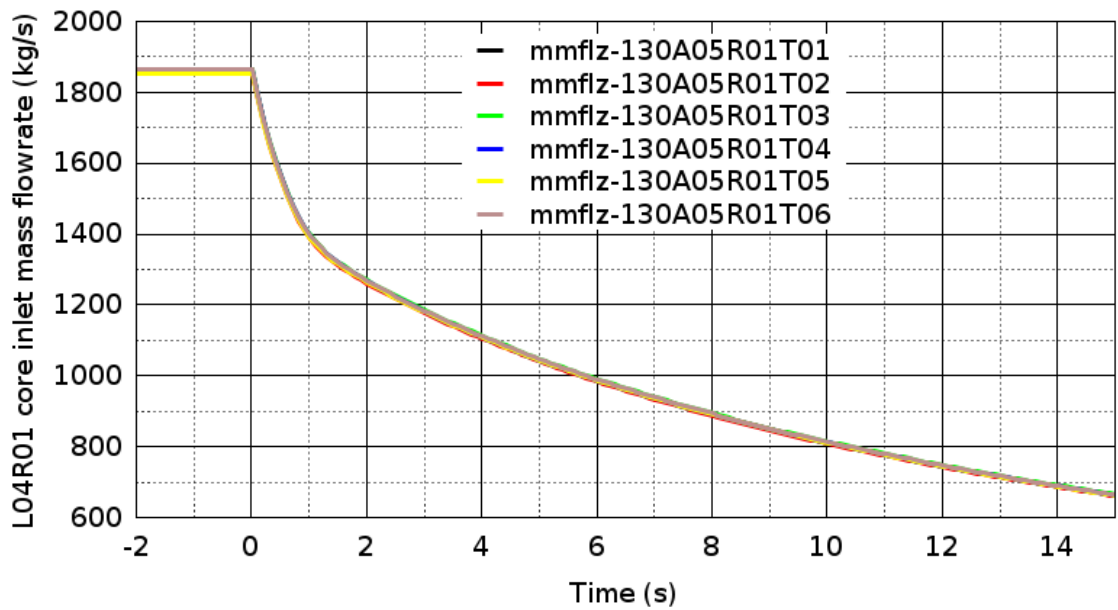**Figure 32. Core inlet pressure in sections R02**
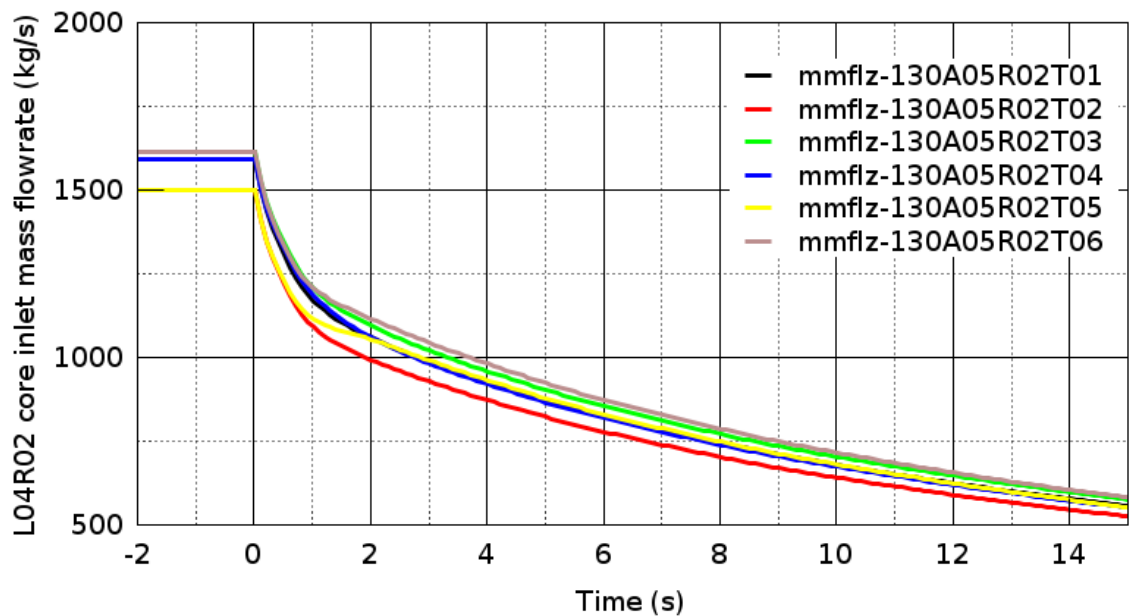
**Figure 33. Core inlet flow rate in sections R01**



**Figure 34. Core inlet flow rate in sections R02**

The next step is to calculate the input parameters for the model of the reactor core created for the subchannel analysis code ALTHAMC12. Figure 28 shows that the ALTHAMC12 reactor core model is identical to sections R01T06, R02T06, and half of sections R01T05 and R02T05 in the TRACE model.

The reactor coolant system pressure and power parameters for all sections change the same as seen in Figures 31 and 32. The core inlet mass flow rate $G_{quarter}$ is calculated by adding the flow of all sections included in the model:

$$G_{quarter} = G_{R01T06} + G_{R02T06} + \frac{(G_{R01T05} + G_{R02T05})}{2}$$
$$= 1864{,}1 + 1614{,}2 + \frac{1854{,}15 + 1500{,}15}{2} = 5155{,}5 \text{ kg/s}$$

where $G_{quarter}$ – inlet mass flow rate of a quarter of the reactor core [kg/s], $G_{R01T06}$, $G_{R02T06}$, $G_{R01T05}$, $G_{R02T05}$ – inlet mass flow rate of the sections [kg/s].

Assumptions and initial conditions for the Reactor Coolant Pump Rotor Seizure are indicated in Table 8.

Table 8. Assumptions and initial conditions for the Reactor Coolant Pump Rotor Seizure

| Core power level, MWt | 995.8 |
|---|---|
| Core inlet coolant temperature, °C | 290.7 |
| Reactor coolant system pressure, MPa | 16.25 |
| Core mass flow, kg/s | 5155.5 |

One of the features of the subchannel analysis code ALTHAMC12 is that it is only able to analyze the model with only one inlet temperature, which will be problematic in case of comparison with sections. Therefore, two comparisons were made – with the inlet temperature of the model which is the quarter of the reactor core, and with the inlet temperature of the section R01T05. This section was chosen because it is here that the biggest changes in parameters occur, it is better suited for validation.

To compare the sections, the parameters of those subchannels that are completely or mostly included in the R01T05 section were taken, as indicated in Figure 35. And the comparison of the outlet reactor coolant temperature as shown in Figure 36.

Despite the inherent disparities in the nodalization approach across models, the results turned out to be similar. Figure 35 shows that not all subchannels are entirely included in the section R01T05, and this, combined with the features of the subchannel analysis code ALTHAMC12 and various assumptions in the calculations, creates a discrepancy. Nevertheless, the behavior of the curves on the graph is identical.
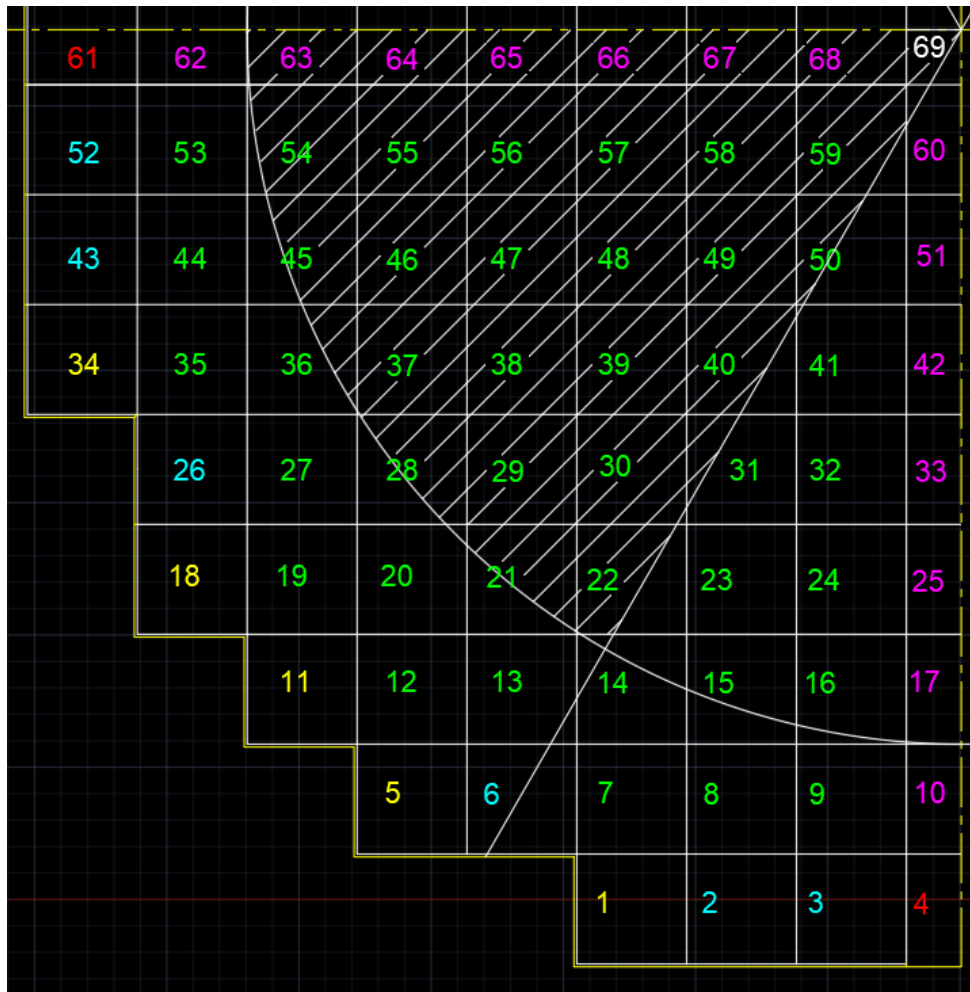
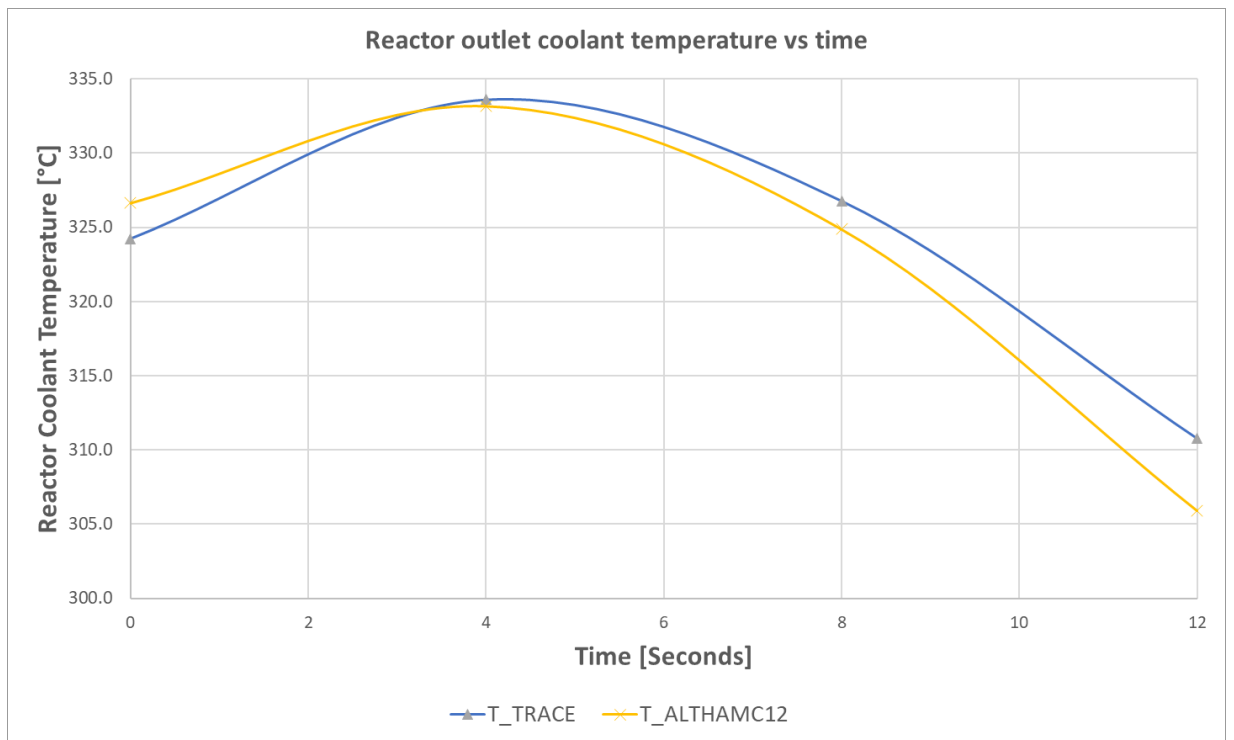**Figure 35. Subchannels belonging to the section R01T05 (shared area)**



**Figure 36. Comparison of the outlet Reactor Coolant Temperature in section R01T05**

This discrepancy is more noticeable when comparing the whole model of the reactor core. The results are shown in Figure 37. The features of the analysis with only one inlet temperature have a significant influence. As well as inconsistencies in the comparison of subchannels and sections. The difference in values between the two comparisons is shown in Figure 38.
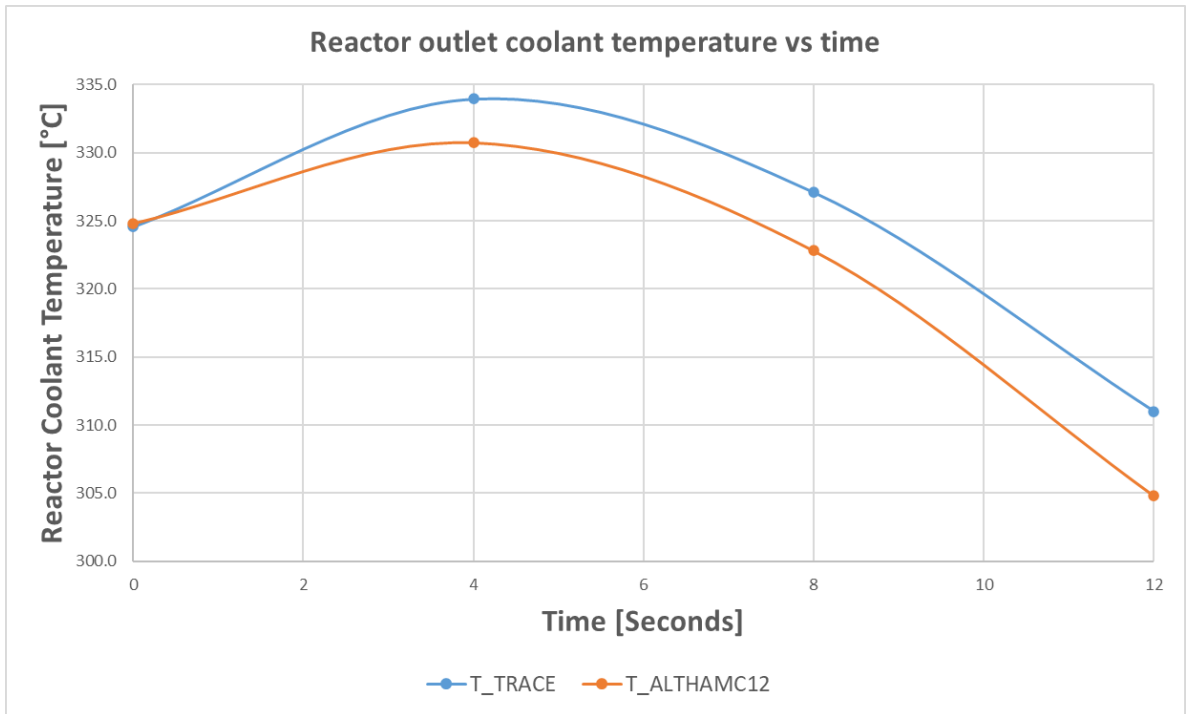


**Figure 37. Comparison of the outlet Reactor Coolant Temperature of the core model**
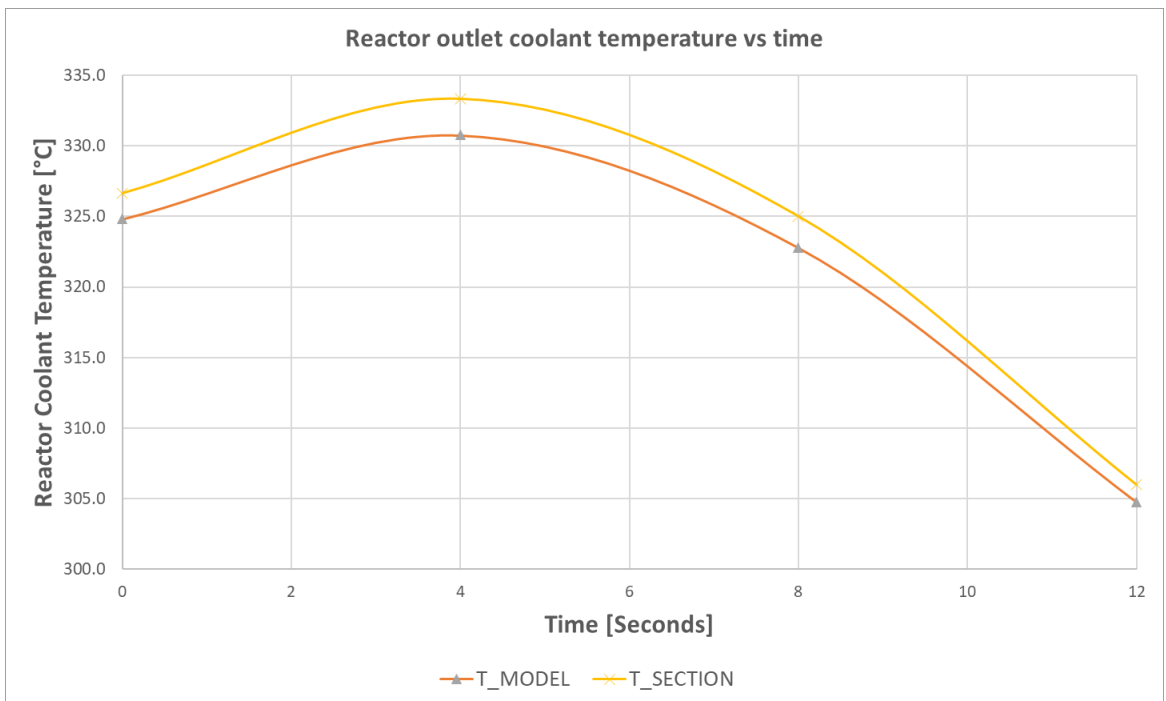


**Figure 38. Difference of the outlet Reactor Coolant Temperature between the two comparisons**

Even in the case of such a discrepancy, the results remain similar enough to say that the core model is created of sufficient quality.

45

# 5. CONCLUSION

The first part of the master thesis presents the general features of the APR1400 reactor and the principles of subchannel calculation methodology using the thermal-hydraulic subchannel analysis code ALTHAMC12.

In the second part of the thesis, the applied knowledge from the theoretical part is used in the analytical part, which includes the analysis of geometric characteristics and physical parameters of the model for the calculation. The result is the creation of an input file generator for subchannel code ALTHAMC12 in MS Excel.

In the third part, the basic principles of verification and validation are described. Model validation consists of four parts. The first part is a comparison of the core general parameters at steady state. In the second part, the base model was supplemented with data and a sensitivity study on inlet flow distribution and validation against coolant outlet properties was carried out. In the third subsection, an analysis of accidents and validation of the average core outlet temperature during Loss of Flow Accident is presented. And in the fourth subsection, validation of the average core outlet temperature during Reactor Coolant Pump Rotor Seizure is shown.

The results of the validation process indicates that the APR1400 reactor model developed with the ALTHAMC12 subchannel analysis code is capable of accurately predicting the reactor's thermal-hydraulic behavior in various operating conditions against the above-mentioned parameters. Thus, this study provides some evidence of the code's reliability and effectiveness as a tool for subchannel analysis of pressurized water reactors, including the APR1400.

# LITERATURE

[1] Korea Electric Power Corporation and Korea Hydro & Nuclear Power Co, Ltd - *APR1400 Design Control Document Tier 2 (APR1400-K-X-FS-14002-NP), CHAPTER 4 - REACTOR* (August 2018) Available from: http://www.nrc.gov/docs/ML1822/ML18228A651.pdf

[2] Kim, Han-Gon - *The Design Characteristics of Advanced Power Reactor 1400* (2011). Available from:

https://pub.iaea.org/MTCD/Publications/PDF/P1500_CD_Web/htm/pdf/topic3/3S09_Hangon%20Kim.pdf

[3] Status report 83 - *Advanced Power Reactor 1400 MWe (APR1400)* (04.11.2011) Available from: https://aris.iaea.org/PDF/APR1400.pdf

[4] *PLUS7 Fuel Design for the APR1400* (November 2012). Available from: https://www.nrc.gov/docs/ML1301/ML13018A139.pdf

[5] KEPCO E&C - KEPCO Engineering & Construction Company, Inc.. (May 2023) [online] Available from: https://www.kepco-enc.com/eng/contents.do?key=1532

[6] *NuScale Power, LLC. Licensting Topical Report. Subchannel Analysis Methodology* (October 2018) [online]. Available from: https://www.nrc.gov/docs/ML1830/ML18305B218.pdf

[7] A. Moorthia, Anil Kumar Sharmab, K. Velusamy - *A review of sub-channel thermal hydraulic codes for nuclear reactor coreand future directions* (April 2018) [online] Available from: https://doi.org/10.1016/j.nucengdes.2018.03.012

[8] BEDNÁŘ, Michal. Subchannel analysis of VVER-1000 reactor core. Brno, 2021. Available from: https://www.vutbr.cz/studenti/zav-prace/detail/134896. Master's thesis. Brno University of Technology, The Faculty of Electrical Engineering and Communication

[9] D. S. Rowe - *COBRA IIIC: a digital computer program for steady state and transient theriyal-hydraulic analysis of rod bundle nuclear fuel elements* (March 1973) [online] Available from: https://www.osti.gov/biblio/4480166-cobra-iiic-digital-computer-program-steady-state-transient-thermal-hydraulic-analysis-rod-bundle-nuclear-fuel-elements

[10] Korea Electric Power Corporation and Korea Hydro & Nuclear Power Company, Ltd., Topical Report APR1400-F-C-EC-13010-NP, *"KCE-1 Critical Heat Flux Correlation for PLUS7 Thermal Design"* (July 2001) [online]. Available from: https://www.nrc.gov/docs/ML1323/ML13239A348.pdf

[11] Hyuk Kwon, K.W. Seo, S. J. Kima, J. P. Park, D. H. Hwang, W.J. Lee b - *Thermal-Hydraulic Design of Mixed Transition Core for FCM Fuel Assembly* (October 2014). Available from: https://www.kns.org/files/pre_paper/32/14A-384%ea%b6%8c%ed%98%81.pdf

[12] Consultation with supervisor Štepán Foral

[13] International Atomic Energy Agency - *Accident Analysis for Nuclear Power Plants* (2002) Available from: https://www-pub.iaea.org/MTCD/Publications/PDF/Pub1131_scr.pdf

[14]    Byung-Jin Lee, Ho-Cheol Jang, Jong-Sik Cheong, Se-Jin Baik - *A Review on the Regionalization Methodology for Core Inlet Flow Distribution Map* (August, 2001) Available from: https://koreascience.kr/article/JAKO200111921634236.pdf

[15]    Autodesk | 3D Design, Engineering & Construction Software (2023) [online]. Available from: https://www.autodesk.com/products/autocad

[16]    Korea Electric Power Corporation and Korea Hydro & Nuclear Power Co, Ltd - *APR1400 Design Control Document Tier 2 (APR1400-K-X-FS-13002-NP), CHAPTER 15 - TRANSIENT AND ACCIDENT ANALYSES* (August 2018) Available from: https://www.nrc.gov/docs/ML1822/ML18228A662.pdf

[17] WebPlotDigitizer - Extract data from plots, images, and maps. Automeris - Analysis tools for engineers and scientists [online]. Copyright © 2010 Available from: https://automeris.io/WebPlotDigitizer/

[18] Data of the model of APR-1400 reactor core from TES s.r.o company, Třebíč; (2023) [online]. Available from: https://www.tes.eu/

[19] K.L. Zhang,V.H. Sanchez-Espinoza - *Coupling of TRACE and SubChanFlow based on the Exterior Communication Interface* (May 2023) [online]. Available from: https://www.sciencedirect.com/science/article/pii/S0149197019301350

# SYMBOLS AND ABBREVIATIONS

Abbreviations:

| | |
|---|---|
| APR | Advanced Power Reactor |
| CEA | control element assembly |
| CEDM | control element drive mechanism |
| DCD | Design Control Document |
| DVI | direct vessel injection |
| ICI | in-core instrumentation |
| IHA | integrated head assembly |
| KAERI | Korea Atomic Energy Research Institute |
| LOFA | Loss of Flow Accident |
| NSSS | nuclear steam supply system |
| OPR | Optimized Power Reactor |
| PWR | pressurized water reactor |
| PZR | pressurizer |
| RCP | reactor coolant pump |
| RCS | reactor coolant system |
| SG | steam generator |
| V&V | verification and validation |

Symbols:

| | | |
|---|---|---|
| $a$ | side of a square | (mm) |
| $ABETA$ | auxiliary coefficient | (-) |
| $\beta$ | turbulent mixing coefficient | (-) |
| $\beta_0$ | turbulent mixing parameter for single-phase | (-) |
| $BBETA$ | auxiliary coefficient | (-) |
| $CBETA$ | auxiliary coefficient | (-) |
| $d_{fr}$ | diameter of the fuel rod | (mm) |
| $d_{fict}$ | diameter of the fictitious rod | (mm) |
| $d_{gt}$ | diameter of the guide thimble | (mm) |
| $f$ | model of the hydraulic resistance of the cross-flow | (-) |
| $G_{quarter}$ | inlet mass flow rate of a quarter of the reactor core | (kg/s) |
| $l$ | length of the boundary | (mm) |
| $l_{fr}$ | distance between fuel rods | (mm) |
| $n$ | number of rows of fuel rods in the fuel assembly | (-) |
| $N_{fr}$ | number of fuel rods | (-) |
| $N_{gt}$ | number of guide thimbles | (-) |
| $P_h$ | heated perimeter | (mm) |
| $P_{fr}$ | perimeter of the fuel rod | (mm) |
| $P_s$ | wetted perimeter | (mm) |
| $q_{diff}$ | difference of the quality fraction | (-) |
| $q_m$ | quality fraction of the model | (-) |

| | | |
|---|---|---|
| $q_{ref}$ | quality fraction from DCD documentation | (-) |
| $Re$ | Reynolds number | (-) |
| $S$ | flow area | (mm$^2$) |
| $S_{square}$ | area of a square | (mm$^2$) |
| $S_{fr}$ | area of fuel rods | (mm$^2$) |
| $S_{gt}$ | area of guide thimbles | (mm$^2$) |
| $T_{HOT}$ | outlet coolant temperature | (°C) |
| $T_{COLD}$ | inlet coolant temperature | (°C) |
| $T_{AVG}$ | average coolant temperature | (°C) |
| $x$ | side of a space between fuel assemblies | (mm) |